

11114692

PERPUSTAKAAN KEJURUTERAAN
UNIVERSITI MALAYA.

**POWER IMPROVEMENT OF WIND TURBINE BASED ON
MAXIMUM POWER POINT TRACKING
(MPPT)CONTROLLER**

ZULINA BINTI ZULKIFELI

**RESEARCH PROJECT SUBMITTED IN PARTIAL
FULFILMENT OF THE REQUIREMENTS FOR THE
DEGREE OF MASTER OF ENGINEERING**

**FACULTY OF ENGINEERING
UNIVERSITY OF MALAYA
KUALA LUMPUR**


2018

Perpustakaan Universiti Malaya



A517447175

UNIVERSITY OF MALAYA
ORIGINAL LITERARY WORK DECLARATION

Name of Candidate: **Zulina Binti Zulkifeli** 

Matric No: **KQC 170004**

Name of Degree: **Master of Engineering (Industrial Electronics and Control)**

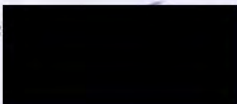
Title of Project Paper/Research Report/Dissertation/Thesis ("this Work"):

**POWER IMPROVEMENT OF WIND TURBINE BASED ON MAXIMUM
POWER POINT TRACKING (MPPT) CONTROLLER**

Field of Study: **CONTROL**

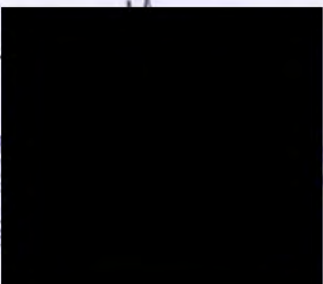
I do solemnly and sincerely declare that:

- (1) I am the sole author/writer of this Work;
- (2) This Work is original;
- (3) Any use of any work in which copyright exists was done by way of fair dealing and for permitted purposes and any excerpt or extract from, or reference to or reproduction of any copyright work has been disclosed expressly and sufficiently and the title of the Work and its authorship have been acknowledged in this Work;
- (4) I do not have any actual knowledge nor do I ought reasonably to know that the making of this work constitutes an infringement of any copyright work;
- (5) I hereby assign all and every rights in the copyright to this Work to the University of Malaya ("UM"), who henceforth shall be owner of the copyright in this Work and that any reproduction or use in any form or by any means whatsoever is prohibited without the written consent of UM having been first had and obtained;
- (6) I am fully aware that if in the course of making this Work I have infringed any copyright whether intentionally or otherwise, I may be subject to legal action or any other action as may be determined by UM.

Candidate's Signature 

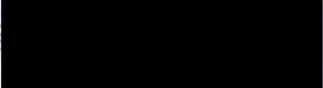
Date: 11-02-2019

Subscribed and solemnly declared before,

Witness's Signature 

Date: 11/2/19

Name: 

Designation: 

POWER IMPROVEMENT OF WIND TURBINE BASED ON MAXIMUM POWER POINT TRACKING (MPPT) CONTROLLER

ABSTRACT

This thesis presents a modern controller for simulation of maximum power point tracking (MPPT) technique using boost converter for wind energy conversion system. It uses output voltage as feedback to regulate its output voltage to a desired value without steady state oscillations with the aid of Matlab ® & Simulink ® simulation software. The methodology is proposed by using modern controller for application of boost DC-DC converter system. It is implemented on the boost converter system by applying state space method. Modern controllers are simulated in closed loop system which consists of state feedback controller, optimal controller, state feedback with feed forward controller and integral controller. These modern controllers are simulated to analyze transient response and percentage of overshoot from boost converter output voltage. If the output system is observable, a full state observer can be implemented. All controllers are compared, which from this work it is proof that state feedback controller at Poles 250x is the best controller, whereby produces less error it is 0.002V error.

PENAMBAHBAIKAN KUASA TURBIN ANGIN BERDASARKAN PENGAWAL PENGESANAN TITIK KUASA MAKSIMUM (MPPT)

ABSTRAK

Tesis ini membentangkan pengawal moden bagi simulasi teknik pengesanan titik kuasa maksimum (MPPT) dengan menggunakan penukar rangsangan untuk sistem penukaran tenaga angin. Ia menggunakan voltan keluaran sebagai maklum balas untuk mengawal voltan keluarannya kepada nilai yang dikehendaki tanpa ayunan keadaan mantap dengan perisian simulasi Matlab® & Simulink ®. Metodologi ini dicadangkan untuk membangunkan pengawal moden bagi aplikasi untuk meningkatkan sistem penukar DC-DC. Kawalan moden dilaksanakan pada sistem dengan menggunakan analisis ruang-keadaan. Simulasi pengawal moden dilakukan dalam sistem gelung tertutup terdiri daripada ruang-keadaan, pengawal optimum, maklum balas keadaan dengan pengawal hadapan suapan dan pengawal integral. Semua kawalan moden ini disimulasikan untuk menganalisis tindak balas sementara dan peratusan lonjakan bagi voltan keluaran pengubah *boost*. Jika keluaran sistem boleh dipantau, maka pemantau keadaan penuh boleh dibangunkan. Semua jenis sistem pengawal dibandingkan dan hasilnya didapati sistem kawalan suap balik ketika pole 250x menghasilkan ralat paling kecil iaitu 0.002V.

ACKNOWLEDGEMENTS

In the name of Allah, The Most Loving and The Most Compassionate. In completing the thesis, I had received helps from many people. They have contributed greatly towards my understanding and thoughts. Firstly, I would like to express my sincere gratitude to my supervisor Dr. Mahidzal Dahari for his encouragement, devoted and committed guidance towards my understanding and thoughts. Utmost gratitude also goes to Ministry of Education (MOE) for the financial support and encouragement to further my study. For my husband, Norhafizul Bin Norawavi, thank you for being my backbone during this challenging period. Special thank also goes to my family and friends. To others who have helped me either directly or indirectly, your help will always be remembered.

TABLE OF CONTENTS

Declaration.....	ii
Abstract	iii
Abstrak	iv
Acknowledgements	v
Table of Contents	vi
List of Figures	x
List of Tables.....	xii
List of Symbols and Abbreviations.....	xiii
List of Appendices	xv
CHAPTER 1: INTRODUCTION.....	1
1.1 Introduction.....	1
1.2 Problem statement	2
1.3 Project objective	3
1.4 Scope of project	3
1.5 Motivation.....	3
1.6 Project organization.....	4
CHAPTER 2: LITERATURE REVIEW.....	6
2.1 Introduction.....	6
2.1.1 Maximum power point tracking control (MPPT).....	6
2.1.2 Hill-climb search (HCS) control	8
2.1.3 Tip speed ratio (TSR)	8
2.1.4 Power to Signal Feedback (PSF).....	8

2.2	Previous research	9
2.3	Research theories	11
2.3.1	Basic block diagram	11
2.3.2	Wind turbine characteristics	12
2.3.3	Boost converter	14
2.4	Mathematical theory	14
2.4.1	Introduction to state space representation	15
2.4.2	Introduction to state space averaging technique	15
2.4.3	Controllability	17
2.4.4	State feedback controller	18
2.4.5	Pole placement technique	19
2.4.6	Optimal control technique	20
2.4.7	State feedback with feed forward controller	21
2.4.8	Integral controller	22
2.4.9	Observability	25
2.4.10	Full state observer	25
2.5	Summary	27
CHAPTER 3: METHODOLOGY		28
3.1	Introduction	28
3.2	Flow of the project	28
3.3	Derivation state space	31
3.4	Analyzing of state space modelling	36
3.5	Analysing of controllability	39
3.6	Analysis of observability	40
3.7	Analysis of poles location	41

3.8	Calculation of state feedback controller	41
3.9	Pole placement technique	42
3.10	Optimal control technique	45
3.11	Calculation of feed forward controller gain.....	46
3.12	Calculation of integral controller gain.....	47
3.13	Calculation of full state observer gain.....	48
3.14	Simulation block diagram.....	50
3.14.1	Wind turbine system.....	51
3.14.2	State feedback controller	54
3.14.3	State feedback with feed forward controller	54
3.14.4	Integral controller.....	55
3.14.5	Comparison of modern controller.....	56
3.14.6	Full state observer	57
3.15	Summary.....	58
 CHAPTER 4: RESULT AND DISCUSSION.....		59
4.1	Introduction.....	59
4.2	Wind turbine system.....	59
4.3	State feedback based on pole placement	60
4.4	State feedback based on optimal control technique.....	62
4.5	State feedback with feed forward controller.....	63
4.6	Integral controller	64
4.7	Comparison of modern controller.....	65
4.8	Result of modern controller.....	66
4.9	Boost converter with full state observer simulation results.....	67
4.10	Summary.....	68

CHAPTER 5: CONCLUSION	69
5.1 Conclusion.....	69
5.2 Recommendation for future work.....	70
REFERENCES.....	71
APPENDIX A.....	73
APPENDIX B.....	74
APPENDIX C.....	75
APPENDIX D.....	76
APPENDIX E.....	78
APPENDIX F.....	79
APPENDIX G.....	80
APPENDIX H.....	81

University of Malaya

LIST OF FIGURES

Figure 2.1: Perturb and observation flowchart.....	7
Figure 2.2: Block diagram of the WECS (Pallavi Behera1, 2015).....	11
Figure 2.3: Turbine power coefficient(Pallavi Behera1, 2015).....	13
Figure 2.4: State space representation.....	16
Figure 2.5: State feedback controller.....	18
Figure 2.6: State feedback with feed forward controller.....	22
Figure 2.7: Integral controller.....	23
Figure 2.8: Full state observer.....	26
Figure 3.1: Flow chart of project methodology.....	30
Figure 3.2: Boost converter circuit.....	31
Figure 3.3: Boost converter when switched closed.....	31
Figure 3.4: The boost converter when it is switched open.....	33
Figure 3.5: Simulink model of wind turbine system.....	51
Figure 3.6: Simulink model of boost circuit.....	52
Figure 3.7: Simulink model of Maximum Power Point Tracking (MPPT).....	53
Figure 3.8: State feedback controller.....	54
Figure 3.9: State feedback with feed forward controller.....	54
Figure 3.10: Integral controller.....	55
Figure 3.11: Comparison of modern controller.....	56
Figure 3.12: Full state observer.....	57
Figure 4.1: Wind turbine boost converter model.....	59

Figure 4.2: Poles placement technique results	60
Figure 4.3: Optimal control technique results	62
Figure 4.4: State feedback with feed forward controller results	63
Figure 4.5: Integral controller result	64
Figure 4.6: Comparison of modern controller	65
Figure 4.7: Boost converter and observer system	68

University of Malaya

LIST OF TABLES

Table 3.1: Boost converter circuit (Pallavi Behera1, 2015).....	36
Table 3.2: Pole placement group.....	42
Table 3.3: State feedback controller gain for designated pole placement.....	44
Table 3.4: Full state observer gain for designated pole placement.....	50
Table 4.1: Requirement parameters of boost converter.....	59
Table 4.2: Analysis result for pole placement technique.....	61
Table 4.3: Modern controller result summary.....	66

LIST OF SYMBOLS AND ABBREVIATIONS

A	:	System state matrix
B	:	Input state matrix
C	:	Output state matrix
CCM	:	<i>Continuous Conduction Mode</i>
CI	:	Capacitor
D	:	Steady state duty cycle
$DDWT$:	<i>Direct Drive Wind Turbine</i>
d	:	Duty cycle
E	:	Feed forward state matrix
e	:	Error
f	:	Switching frequency
i_{cl}	:	Capacitor current
i_L	:	Inductor current
I_{max}	:	Maximum current
I_{min}	:	Minimum current
i_o	:	Current output
i_{RL}	:	Load current
K	:	Controller gain
L	:	Observer gain
L_{min}	:	Minimum inductor
LI	:	Inductor
Mc	:	Controllability matrix

M_o	:	Observability matrix
$MPPT$:	<i>Maximum Power Point Tracking</i>
N	:	Feed forward
P	:	Pole
Q	:	State weighting matrix
R	:	Input weighting matrix
R_L	:	Load
T	:	Period of switching frequency,s
T_s	:	Setling time
u	:	Input
V_{cl}	:	Capacitor voltage
V_{Ll}	:	Inductor voltage
V_i	:	Input voltage
V_o	:	Output voltage
V_{sw}	:	Pulse voltage
\hat{v}	:	Integral input
$WECS$:	<i>Wind Energy Conversion System</i>
x	:	Steady-state variable
\dot{x}	:	State variable
\hat{x}	:	Estimated state variable
y	:	Output
\hat{y}	:	Estimated output

LIST OF APPENDICES

APPENDIX A: M-FILE FOR BOOST CONVERTER SYSTEM

APPENDIX B: M-FILE FOR CONTROLLABILITY & OBSERVABILITY

APPENDIX C: M-FILE FOR DETERMINE EIG A

APPENDIX D: M-FILE FOR POLES LOCATION

APPENDIX E: M-FILE FOR OPTIMAL CONTROLLER

APPENDIX F: M-FILE FOR FEED FORWARD CONTROLLER

APPENDIX G: M-FILE FOR INTEGRAL CONTROLLER

APPENDIX H: M-FILE FOR OBSERVER

CHAPTER 1: INTRODUCTION

This chapter explains the overview of the introduction, problem statement, objective, scope, motivation and project organization.

1.1 Introduction

Nowadays, one of the assorted renewable energy sources which is wind has emerged as an able contender, additional alone to solar energy. Wind energy designed to convert the wind energy into electric energy. Wind energy is favored in light of the fact that it is spotless, contamination free, expendable and secure (Vinod & Sinha, 2014).

Among the electric generators, permanent magnet synchronous generator (PMSG) is adopted due its aerial efficiency, reliability, ability density, ablaze weight and self-excitation features. Controlling PMSG to accomplish the maximum power point (MPP) can be done by changing its load. (Abdullah, Yatim, Tan, & Saidur, 2012). The performance of various speed and the desired maximum energy output can be compare by using the maximum power point tracking (MPPT) algorithm. Thus, the implementation with boost converter by controlling the duty cycle of the converter the apparent load seen by the generator will adjust its output voltage and shaft speed.

Besides that, it provides information for the design of the compensator. The most common modelling method for the converter is matrix-based technique. This state-space approach is a time domain model where the system is described by differential or difference equation. It greatly allows simplified mathematical representation of the system which is vector-matrix differential equation. This proeses great advantage because it particularly suited for digital computer implementation due to their time-domain approach and vector matrix description. The modelling of dynamic model of Maximum

Power Point Tracking (MPPT) for wind energy system by using boost converters and state space approach would be explained in Chapter 3.

1.2 Problem statement

Wind energy can be amply found in our surrounding. However, its abrupt change nature poses major drawback to the wind energy conversion system (WECS). The drawback problem can be overcoming by implementation of control action like Maximum Power Point Tracking (MPPT) control. This control strategy allows to achieve the maximum power at any wind speed since the characteristic of the wind turbine is non-linear. Hence, the efficiency of the wind turbine module is very low and the power DC load output depends on wind turbine mechanical movement. To achieve maximum power at any wind speed, it is commonly implemented through boost converter.

DC output voltage of boost converter can vary depending on the application requirement. In any case, usually its output value is distorted because of oscillation, poor settling time and high steady-state error. Consequently, it causes negative effect on the transient response and reduce the general output voltage execution. Therefore, a controller needs to be developed in order to overcome mentioned issues. A modern controller that is based on state feedback controller, optimal controller, observable controller, state feedback with feed forward controller and integral controller is suggested to accomplish quickest transient response with no overshoot.

1.3 Project objective

The objectives of this project are as listed below:

- To design and simulate a model of modern controller via Matlab® and Simulink for the improvement of wind turbine.
- To compare steady state, settling time, percentage overshoot and steady state error of modern controllers and observer with original boost system
- To propose a modern controller for boost converter of wind turbine

1.4 Scope of project

The focus of this research is to monitor the output voltage of boost converter model. The MPPT technique is required to obtain maximum power point for voltage of wind turbine system.

The modern controller theories are applied in this project and they are only based on Matlab® & Simulink® simulation approach.

In particular, this project is done to find a controller that can provide fastest settling time, minimum percentage of overshoot and steady-state error ≤ 1 .

1.5 Motivation

Conventional controls such as PI and /or PID controller, fuzzy and neural network has been applied to regulate the output voltage to desired value in current boost converter. Nonetheless, because of certain limitations, this regular method results in complex mathematical model, which is difficult to deal with. Therefore, as an alternative, state feedback controller, optimal controller, state feedback with feed forward controller and integral controller are suggested to reduce the complexity of the controller design. Since

it is time domain based, fast transient response with desired value is achievable. A full state observer is also applied to show that all initials state can be resolved.

1.6 Project organization

The project consists of five chapter. It is coordinated as follows:

Chapter 1: Introduction

This chapter gives overview of this project. It consists of introduction to the project, problem statement, objective, scope, motivation and project organization.

Chapter 2: Literature Review

In this chapter, introduction of wind turbine, MPPT, boost converter, theory of modern controller and observer are explained in details. Additionally, previous works by other researchers on similar subject are discussed to provide information on the current state of the technology.

Chapter 3: Methodology

Explanation on derivation of state space averaging technique, boost converter state space derivation and modelling are given. Furthermore, description on controllability and observability, analysis of poles location, controller gain and analysis of modern controller via Matlab® & Simulink® software are provided as well.

Chapter 4: Results and Discussion LITERATURE REVIEW

This chapter discusses on controller simulation results based on steady state, settling time, percentage of overshoot and steady-state error whilst observer is investigating the original boost system of the output voltage.

Chapter 5: Conclusion

In this final chapter, conclusion of the overall research project findings is presented. Suggestion for modern controller's techniques and improvements and recommendations for further research is specified.

CHAPTER 2: LITERATURE REVIEW

In this chapter, introduction of MPPT technique using boost converter for Wind Energy Conversion System (WECS), theory of modern controller and observer are explained in details. Additionally, previous works by other researches on similar subject are discussed to provide information on current state of the technology.

2.1 Introduction

An ideal converter converts the DC output voltage, V_o to a different level and delivers it as regulated output. Furthermore, V_o should be adjusted according to application's requirement. However, the desired output voltage is not always achievable in practical. The input voltage of the particular system should be helped by using switching technique. There are two switching modes available for selection, namely switch close mode or switch open mode respectively. Value of V_o also depends on the steady state duty cycle, D of the switching frequency. Additionally, feedback controller is applied to the boost controller to rectify error at V_o automatically and to ensure output voltage is at the desired level. The combination of these components has resulted in the built of modern controllers (Abdullah et al., 2012). However, the modern observer also include in this implementation since there are unknown parameter in the system.

2.1.1 Maximum power point tracking control (MPPT)

Due to problems like the depletion of fossil fuel reserves and concerns about the consequences of the usage of fossil fuel and nuclear energy source towards the environment. Wind generation system as a renewable energy source had been attracting

wide attention. Nevertheless, although wind energy is abundant and can be easily found, it varies continually owing to the wind speed changes throughout the day. Amount of power output from wind energy conversion system (WECS) depends upon the accuracy in which the peak power points are tracked by the MPPT controller of the WECS control system irrespective of the type of generator used. The perturb and observation algorithm is used in the MPPT modelling. Figure 2.1 shows that the flow chart logic of perturb and observation algorithm will apply.

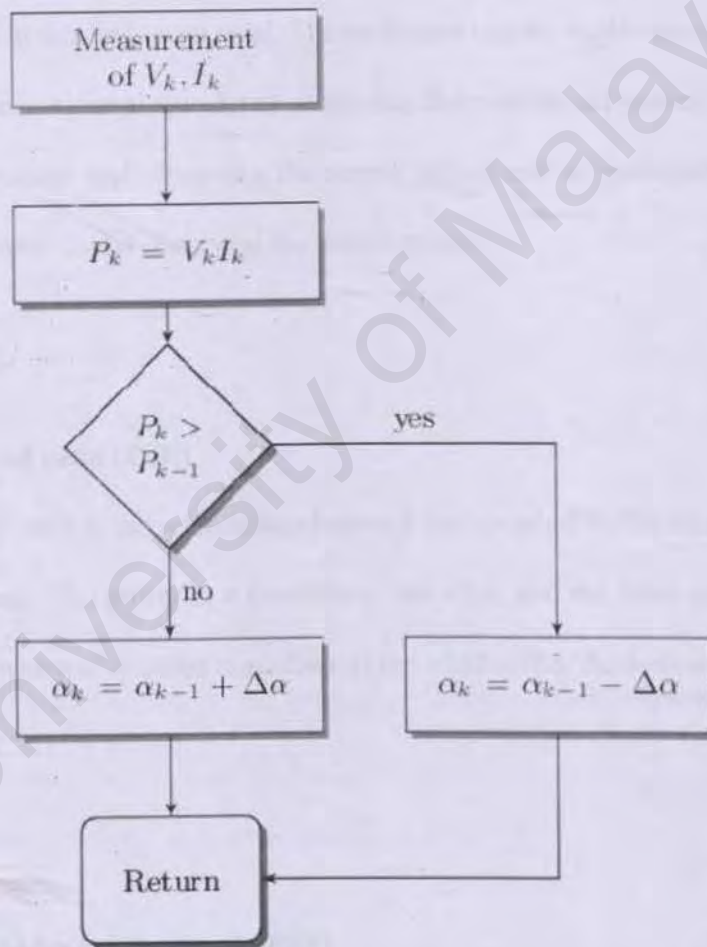


Figure 2.1: Perturb and observation flowchart (Pallavi Beheral,2015)

Currently, MPPT have three control methods to extract the maximum power which are hill-climb search (HSC) control, tip speed ratio (TSR) control and power signal feedback (PSF) control respectively.

2.1.2 Hill-climb search (HCS) control

HCS technique tracks this point by comparing the previous and actual power in the curve making variations of a decided variable. Perturbation and observation are the most parameters used in this technique used. The technique can be implemented in three ways by perturbing the rotational speed and observing the mechanical power, perturbing the inverter input voltage and observing the output power and by perturbing the DC-DC converter duty cycle D and observing the output power.

2.1.3 Tip speed ratio (TSR)

The tip speed ratio is the relationship between the speed of the turbine blade and the speed of the wind. The power is a function of the wind and the rotor speed. When the TSR is optimal which is constant regardless of the wind speed, the derived energy will be amplified.

2.1.4 Power to Signal Feedback (PSF)

The reference obtained from simulations or experimental tests will be the curve of rotational speed versus optimal power. To implement PSF technique, the maximum power is tracked by the shaft speed measurement and power reference. The method is

does not require the measurement of wind velocity. However, the drawback is the requirement of mechanical shaft speed and wind turbine output power measurement.

2.2 Previous research

(Odgaard, Hovgaard, & Wiesniewski, 2016) have proposed the operation of a wind turbine to stabilize the grid. The energy tally achieves maximum when following temporary boost commands for power distributed to the grid. More, it also limits on the rotor speed and generator power preceding a boost. This paper exhibits how a natural plan can control the turbine amid the lift and the resulting recuperation stage to such an extent that the dynamic vitality put away in the breeze turbine rotor is not to depleted to the basic low level. The research also has provided a widespread closed loop test with an industrial wind turbine simulator.

An experimental comparative study for three phase single stage boost inverter for direct drive wind is presented by (Singh & Mirafzal, 2016) in their research paper. The paper has suggested a power electronics interface topology for direct drive wind turbines (DDWT) to enhance the framework dependability and with possibility to diminish the extent of the permanent magnet (PM) generator. In the proposed topology, the matrix side voltage source converter in a conventional DDWT is supplanted by a three-stage single arrange help inverter. It will empower the utilization of a low-voltage generator and along these permits plan of a littler measured generator. A definite unwavering quality examination current power electronic interface alongside that of the created interface is introduced. The legitimacy of the proposed framework is bolstered by a set of Matlab/Simulink re-enactments on the shut circle network tied system.

(Eviningsih, Putri, Pujiantara, Priyadi, & Purnomo, 2017) have evaluated the major problem of wind turbine systems which is to get the greatest power yield and to keep up the DC voltage at a constant value through the breeze variance. The paper has proposed method uses the output voltage and current of a rectifier to determine the duty cycle of the boost converter, without requiring the wind speed information and turbine characteristics. Besides that, maximum power extraction controller has a simple structure, low cost and a good response for various of wind speed. Thus, achieve a higher maximum power at 93.87% of an accuracy.

(Trejos-Grisales, Guarnizo-Lemus, & Serna, 2014) which evaluates the general overview of the main characteristics of the wind power systems, with the consideration on the simulation models and the most used Maximum Power Point Tracker (MPPT) techniques are made. Other than that, some simulation results are shown and conclusion about the work had been done.

(Kumar & Chatterjee, 2016) have reviewed merit, demerits and comprehensive comparison of the different MPPT algorithms also highlighted in the terms of complexity, wind speed requirement, prior training, speed responses and the maximal energy output. This paper serves as a proper reference for future MPPT users in selecting appropriate MPPT algorithm for the requirement.

(Jeong, Seung, & Lee, 2012) have proposed method to improved the maximum power point tracking method for wind power system. Two combination method are proposed using TSR and Hysteresis control. The result has shown that the controller does not interfere with each other and they provide excellent performance.

2.3 Research theories

This section explains about the theory of wind turbine system modelling, maximum power point tracking (MPPT) modelling and DC-DC boost converter which consists of state space representation, state feedback controller, optimal controller, state feedback with feed forward controller, integral controller and full state observer. Mathematical theory of each controller is also discussed in details.

2.3.1 Basic block diagram

Figure 2.2 shows the block diagram of the proposed system for applying MPPT method. A DC/DC boost converter is used at the output terminals of the rectifier. MPPT control signal is given to the boost converter which will accordingly boosts up the voltage across the load resistor. A PWM bridge inverter is used at the load side. The main purpose of the rectifier is to deliver a DC voltage signal to the converter, so some control action can be made.

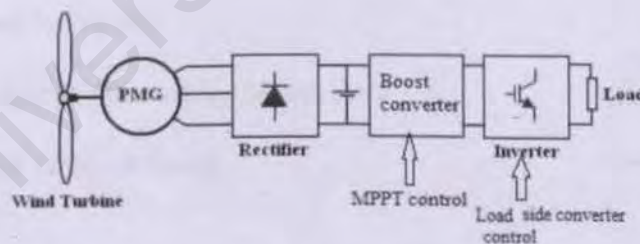


Figure 2.2: Block diagram of the WECS (Pallavi Behera1, 2015)

2.3.2 Wind turbine characteristics

Wind turbines convert the kinetic energy present in the wind into mechanical energy by means of producing torque which is injected to a generator. Three main parts of wind energy system are the rotor, generator and structure. The three indicators that vary with the wind speed which characterize the performances of a wind turbine are power, torque and thrust.

The power contained in wind P_{wind} is listed as below;

$$P_{wind} = \frac{1}{2} \rho AV^3 \quad (2.1)$$

Power extracted by the wind turbine P_m is

$$P_m = \frac{1}{2} \rho AV^3 C_p(\lambda, \beta) \quad (2.2)$$

Where;

P_m = Mechanical power in the moving air (Watt)

ρ = Air density (kg/m³)

A = Area swept by the turbine blades (m²)

V = Velocity of the air (m/s)

Where C_p is the turbine coefficient. It is a transcendental function of blade pitch angle (β) and the tip speed ratio (λ).

$$C_p = 0.5 \left(\frac{116}{\lambda_i} - 0.4\beta - 5 \right) e^{\frac{21}{\lambda_i}} + 0.0068\lambda \quad (2.3)$$

$$\frac{1}{\lambda_i} = \frac{1}{\lambda} - 0.035 \quad (2.4)$$

$$\lambda = \frac{\omega R}{V} \quad (2.5)$$

Where, ω is the rotor speed, R is the turbines radius. β is fixed by the shape of turbines blades. Thus C_p can be expressed as a function of λ only. A typical $C_p(\lambda)$ curve is shown in figure 2.3.

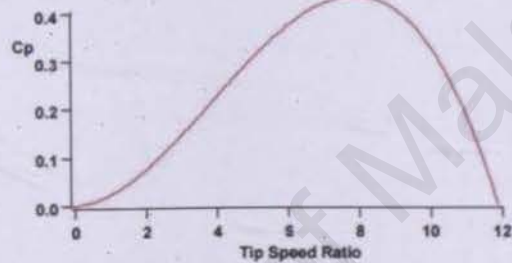


Figure 2.3: Turbine power coefficient(Pallavi Behera1, 2015)

Power output of the generator P_G ;

$$P_G = \eta P_m \quad (2.6)$$

Where η is the generator efficiency.

Using the relation (2.2) – (2.6) it can be inferred that at any particular wind speed, the generator outputs maximum power at a specific rotor speed. By controlling the duty ratio of the intermediate boost converter, the load resistance referred to the generator terminals is varied along with the changes in wind, such that maximum power is extracted continuously.

2.3.3 Boost converter

Boost converter known as a step-up converter is placed to obtain maximum output and always greater than input. It able to step up the voltage without a transformer. Boost converter can be operated by close or open the switch depend on the output requirement. The output voltage to the load or resistor must always be greater than the input voltage. Boost converter provides high efficiency due to a single switch in the circuit.

$$V_0 = \frac{1}{1-D} V_1 \quad (2.7)$$

The values for the various components of the boost converter are calculated using the following equations

$$L = \frac{V_1(V_0-V_1)}{\Delta I_L f_s V_0} \quad (2.8)$$

$$\Delta I_L = (0.2 \text{ to } 0.4) I_o \frac{V_0}{V_1} \quad (2.9)$$

$$C_{min} = \frac{I_o D}{f_s \Delta V_o} \quad (2.10)$$

Where, V_1 is the input voltage, V_0 is the output voltage, I_o is the output current, D is the duty ratio, L is the inductance, C_{min} is the minimum value of capacitance required, ΔI_L is the ripple current, f_s is the switching frequency.

2.4 Mathematical theory

This section explains in detail about theory of state space representation, state feedback controller, optimal controller, state feedback with feed forward controller, integral

controller and full state observer. More, mathematical theory of each controller and observer are also discussed in details.

2.4.1 Introduction to state space representation

Modern control theory or also referred to as state space analysis is a method for modelling, analyzing and designing a wide range of systems. These systems can typically be described by differential equations. The advantage of state-space analysis is that it is applicable on non-linear system as well as MIMO systems. A state space analysis is easily computed using advanced digital computer program such as Matlab® software. However, before one can proceed to create model and simulate the DC-DC converter, it is essential to obtain the appropriate state space equation first (Yaramasu, Wu, Sen, Kouro, & Narimani, 2015).

2.4.2 Introduction to state space averaging technique

State space averaging is a generic method in which circuit that changes over a switching period are described.

$$\dot{x} = Ax + Bu \quad (2.11)$$

$$y = v_o = Cx + Eu \quad (2.12)$$

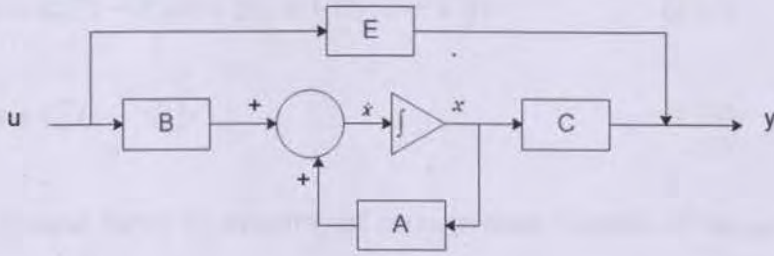


Figure 2.4: State space representation

Where A is called the state matrix, B the input matrix, C the output matrix, u is input and y is output. A block diagram represented of Equations 2.11 and 2.12 is shown in Figure 2.4 (Ogata, 2010).

Within this project, $E = [0]$ and thus will be ignored for mathematical analysis. However, in Matlab m-file analysis, D is represented as E since the capital D is not used with Matlab commands.

In case of a switch closed-model, following equations are implemented:

$$\dot{x} = A_1 x + B_1 u \quad (2.13)$$

$$v_o = C_1^T x \quad (2.14)$$

When it is switch open model, below equations are implemented

$$\dot{x} = A_2 x + B_2 u \quad (2.15)$$

$$v_o = C_2^T x \quad (2.16)$$

Time dT represents switch closed while $(1-d) T$ represents switch open and weighted average equations is given below,

$$\dot{x} = [A_1 x + A_2(1 - d)]x + [B_1 x + B_2(1 - d)]u \quad (2.17)$$

$$v_o = [C_1^T x + C_2^T(1 - d)]x \quad (2.18)$$

Thus, the general forms to describe an average state-variable of the system are as shown below,

$$A = A_1 d + A_2(1 - d) \quad (2.19)$$

$$B = B_1 d + B_2(1 - d) \quad (2.20)$$

$$C = C_1^T x + C_2^T(1 - d) \quad (2.21)$$

2.4.3 Controllability

Controller is designed to allow dedicated system to sustain its output voltage. Hence, due to its role as one of the controller's major component, boost converter needs to be administrable to ensure that the system's state space can derived.

The controllability matrix M_c is constructed from matrices A and B as shown below in Equation 2.22.

$$M_c = [B \ AB \ \dots \ A^{n-1} B] \quad (2.22)$$

In above equation, n is the order of the system. The system is only fully controllable if M_c is a full rank matrix, which means that the determinant of M_c is not allowed to be zero. Otherwise, the system is no longer controllable.

2.4.4 State feedback controller

The first step in designing a state variable requires the assumption that all states are variable for feedback and they are able to access complete state $x(t)$ for all t . system input $u(t)$ is given by below equation:

$$u = -Kx \quad (2.23)$$

Determining the gain matrix K is the objective of state feedback design process. Figure 2.5 shows block diagram of a state feedback controller, where K is feedback gain.

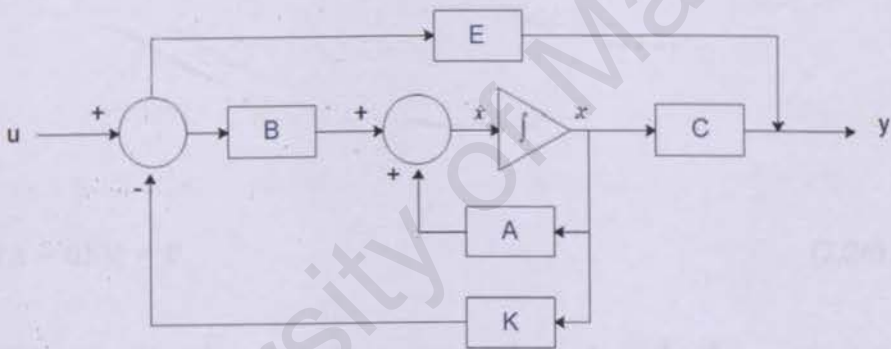


Figure 2.5: State feedback controller

As derived from the above circuit model, a closed loop system equation is

$$\dot{x} = (A - BK)x \quad (2.24)$$

$$y = (C - EK)x \quad (2.25)$$

Next, pole placement and optimal control technique will be presented to determine the feedback gain matrix K .

2.4.5 Pole placement technique

The full state variable feedback control technique is a technique in which the concept of feeding of all state variables back into the admission of a system via a fitting feedback matrix in the control strategy. Via this method, the aimed location of the closed loop eigenvalues (poles) of the system will be specified. For this research purposes, the design of a feedback controller that is capable of moving some or all of the open loop poles of the measured system to the specified close loop pole location is being aimed. This method is commonly known as the pole placement control design and it is utilized in controller design due to its ability to bring system stability, set point tracking and reject disturbance.

For state feedback controller, the closed loop characteristic can be determined by (Ogata, 2010)

$$|\lambda I - (A - BK)| = 0 \quad (2.26)$$

In order to determine the value of gain matrix K, the desired poles need to be placed. The number of desired poles depends on the system order. For a system that has an n-order, the poles are n, and the characteristic equation can be written as show below (Ogata, 2010)

$$(s - p_1)(s - p_2) \dots \dots (s - p_n) = 0 \quad (2.27)$$

Matrix K can then be determined by comparing coefficients between characteristic in Equation 2.26 and 2.27 and the value is used in Figure in the previous page. In addition,

matrix K also can be determined by using matrix A in Matlab® & Simulink command as shown below in Equation 2.28(Ogata, 2010)

$$\text{eig}(A) \quad (2.28)$$

2.4.6 Optimal control technique

The design of optimal control is paramount in control engineering. The design is utilized to accomplish a system with practical components that is capable of producing aspired operating performance in the future. Systems that are adjusted to provide minimal performance index are commonly addressed as optimal control system. It is accomplished through the adjustment of the system parameters so that the index reaches an extreme value, which is typically a minimum value.

Via this approach, the stability in the system is achieved through the determination of feedback gain matrix that minimizes J . The mathematical equation is as follow (Ogata, 2010).

$$J = \int_0^{\infty} (x^T Q_x + u^T R u) dt \quad (2.29)$$

In Equation 2.30, matrix Q can be derived as follows:

$$Q = C^T C \quad (2.30)$$

The value of Q and R are definite positive and in order to solve optimization problem over a finite time interval, algebraic Ricatti equation is the most frequently used(Ogata, 2010).

$$A^T P + P A - P B R^{-1} B^T P + Q = 0 \quad (2.31)$$

$$K = R^{-1} B^T P \quad (2.32)$$

In the above equations, P is symmetric, positive definite matrix and K is the optimal gain that is used in state feedback controller design.

In the next section, state feedback with feed forward controller will be explained.

2.4.7 State feedback with feed forward controller

State feedback with feed forward controller can be substantially enhance the result of state feedback output during major measurable disturbance occurrence before it alters the output process. Furthermore, it is capable of completely eliminating the effect that measured disturbances pose on the process output. The calculation of the state feedback controller gain, K is explained in previous subchapter 2.6, whereas the feed forward gain, N is calculated as shown below in Equation 2.33. the matrix value of the system is substituted in below equation, where I is the identify matrix (Ogata, 2010).

$$\begin{bmatrix} N_x \\ N_u \end{bmatrix} = \begin{bmatrix} A & B \\ C & E \end{bmatrix}^{-1} \begin{bmatrix} 0 \\ 1 \end{bmatrix} \quad (2.33)$$

The result is divided into values, namely one for scalar N_u and another one for N_x in matrix form. Then, Equation (2.34) is used to calculated N value, where K value is as calculated in state feedback controller system.

$$N = N_u + KNx \quad (2.34)$$

Figure 2.6 shows the block diagram for state feedback with feed forward controller block diagram (Ogata, 2010).

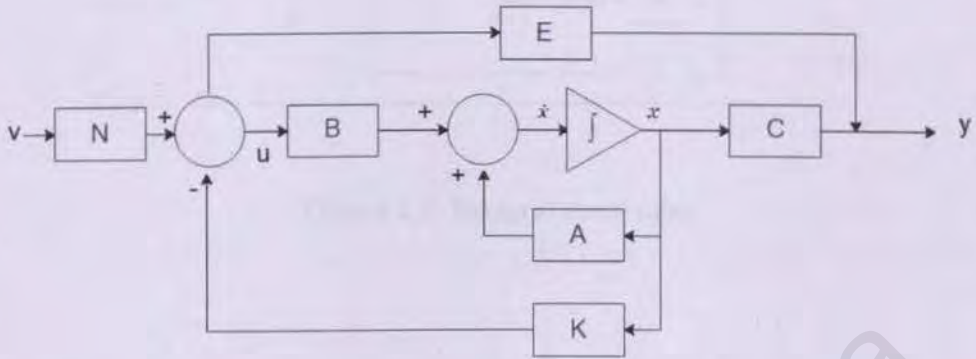


Figure 2.6: State feedback with feed forward controller

2.4.8 Integral controller

A frequent main disadvantage that take place in the midst of the design phase of a state feedback controller by using pole-placement is large offset. Consequently, integral control is added to oust the offset in the response to the step input. Additionally, the integral control can also add value to the robustness of the system. The value gain, K comes from outside the feedback loop. The overall system is quite sensitive to outside elements such as noise or disturbance. Therefore, both integral control and state feedback with feed forward controller will unify their functions to achieve robustness from these external disturbances. The block diagram of an integral controller shown in Figure 2.7.

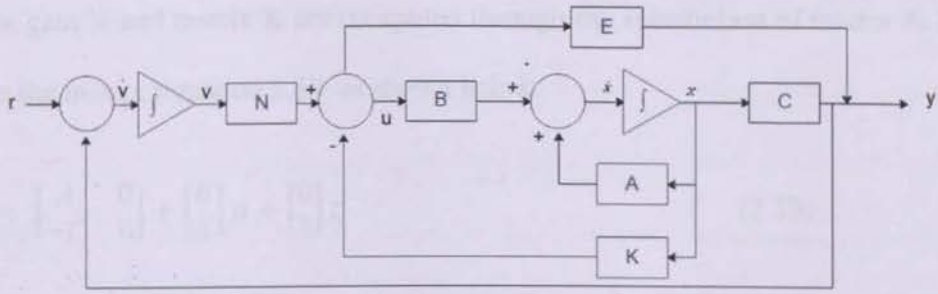


Figure 2.7: Integral controller

The controller state space's mathematical models are represented as follows:

$$\dot{x} = Ax + Bu \quad (2.35)$$

$$\dot{v} = -Cx - Eu + r \quad (2.36)$$

$$u = -[K - N] \begin{bmatrix} x \\ v \end{bmatrix} \quad (2.37)$$

$$y = Cx + Eu \quad (2.38)$$

Where,

\dot{x} = state variable

\dot{v} = integral input

u = state feedback with feed forward controller

y = output

The new gain N and matrix K are computed through the substitution of matrix A , B , C and E in the matrix Equation 2.39. as shown below:

$$\begin{bmatrix} \dot{x} \\ \dot{v} \end{bmatrix} = \begin{bmatrix} A & 0 \\ -C & 0 \end{bmatrix} + \begin{bmatrix} B \\ E \end{bmatrix} u + \begin{bmatrix} 0 \\ 1 \end{bmatrix} r \quad (2.39)$$

Result from equation 2.39 will produce a new matrix A and B . Next the value for system K is derived from following equation:

$$K = [K_1 \quad K_2 \quad -K_3] \quad (2.40)$$

After that, the substituted characteristic polynomial is compared to the desired eigenvalue by using Equation 2.26 and 2.27 and K value can also be determined. The value of $-K_3$ is the forward gain and the value of K_1 and K_2 is the feedback gain. The equations are follows:

$$N = -K_3 \quad (2.41)$$

$$K = [K_1 \quad K_2] \quad (2.42)$$

When enforced in this controller, the compensated system becomes Equation 2.43 as shown below:

$$\begin{bmatrix} \dot{x} \\ \dot{v} \end{bmatrix} = \begin{bmatrix} A - BK & BN \\ -C & 0 \end{bmatrix} + \begin{bmatrix} x \\ v \end{bmatrix} u + \begin{bmatrix} 0 \\ 1 \end{bmatrix} r \quad (2.43)$$

2.4.9 Observability

Observer is a dynamic system utilized to evaluate the state of another dynamic system. It gives feedback given knowledge of the system inputs and measurements of the system outputs. In order to see what is going on inside the system under observation, the system must be observable at the first place. A system is completely observable $y(t)$ given the control $u(t)$, $0 \leq t \leq T$.

The system is entirely observable when this is true regardless of the initial time and state. The observability matrix, M_o is constructed from matrix A and C in the following matrix.

$$M_o = \begin{bmatrix} C \\ CA \\ \vdots \\ CA^{n-1} \end{bmatrix} \quad (2.44)$$

Where n is the order of the system. The system is fully observable if matrix M_o is a full rank. In other word, the system is completely observable when the determinant of the observability matrix M_o is non-zero. Besides, the system is also detectable when it is completely observable.

2.4.10 Full state observer

Observer is used to estimate states of a system. The same pole-placement techniques as used in controller design can be used. Poles of the observer were changed deliberately to test how the performance of the observer varied.

Figure 2.8 illustrates how the observer estimates the states of the system. $\dot{\hat{x}}$, \hat{x} and \hat{y} represents the estimated values. The output \hat{y} is compared to the output of the system. If any differences are found from the comparison, it will be multiplied with an observer matrix gain, L and feedback to the state estimator dynamics.

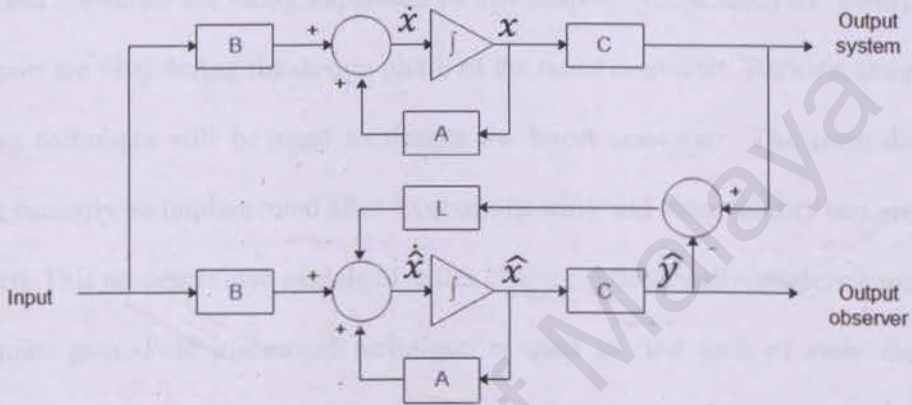


Figure 2.8: Full state observer

The calculation of full state observer is:

$$\dot{x} - \dot{\hat{x}} = (A - LC)(x - \hat{x}) \quad (2.45)$$

The characteristic equation of the full state observer system can be derived from:

$$|sI - (A - LC)| = 0 \quad (2.46)$$

2.5 Summary

Modern control method is used to analyze the performance of boost converter by using state feedback controller, optimal controller, state feedback with feed forward, integral controller and full state feedback observer. These methods have been used previously by many of researchers. In this chapter, some of the earlier researches work conducted by researchers all around the globe is presented. Then, background theories about boost converter are being explained in this chapter. These theories' contribution and support are vital during the design phase of the boost converter. Besides, state space averaging technique will be used to design the boost converter. The controller and observer can only be implemented after its controllability and observability test are being conducted. This process is also explained in this chapter. Additionally, modern controllers also require gain. Pole placement technique is used to find gain of state feedback controller. From this finding we choose modern controller analysis to improve settling time and overshoot in Chapter 3.

CHAPTER 3: METHODOLOGY

Explanation on derivation of state space averaging technique, boost converter state space derivation and modelling are given in the chapter. Description on controllability and observability, analysis of poles location, controller gain and analysis of modern controller via Matlab® & Simulink® software are provided as well.

3.1 Introduction

Based on the overview of converter controllers that are presented in previous chapter, it is found that there are less studies conducted on boost converter by using modern controllers. It is found that only PI, PID and fuzzy controller as used as a controller. It is hoped that this project could serve as valuable source for future, researchers and developers of modern controller for boost converter.

3.2 Flow of the project

There are five different phases implemented within this project. In the next page, Figure 3.1 shows the flow chart of the project methodology. It started with mathematical modelling, then it continues with controllability and observability characteristic. The next step is to determine poles location before analyzing with simulation and analysis result. In mathematical modelling phase, state space of boost converter is derived and defined. Besides that, minimum current flow through inductor is also verified. As the next step, state space equations are used to check the controllability and observability of the boost converter. The poles locations are determined after the system is found to be controllable and observable. These poles location is used to find gain in modern controllers and

observer. In order to simulate both modern controller and observer, their gains value are inserted into respective Simulink model. During verification and validation phase, results from open loop and closed loop boost converter are analyzed. Finally, the results are compared and discussed to determine finalize the best controller performance.



Figure 2.1. Block diagram of boost converter control system

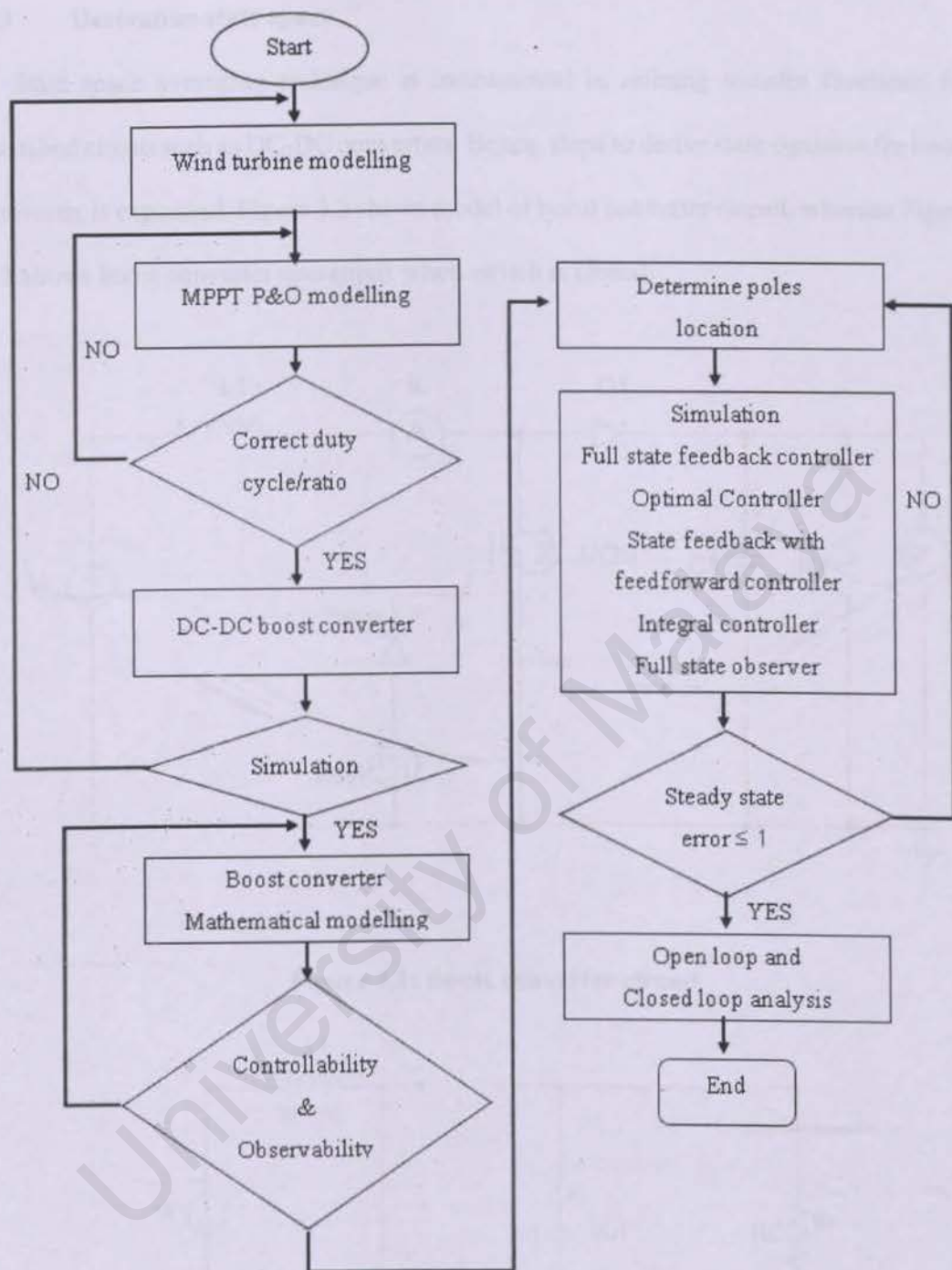


Figure 3.1: Flow chart of project methodology

3.3 Derivation state space

State space averaging technique is instrumental in refining transfer functions for switched circuit such as DC-DC converters. Hence, steps to derive state equation for boost converter is explained. Figure 3.2 shows model of boost converter circuit, whereas Figure 3.3 shows boost converter operations when switch is closed.

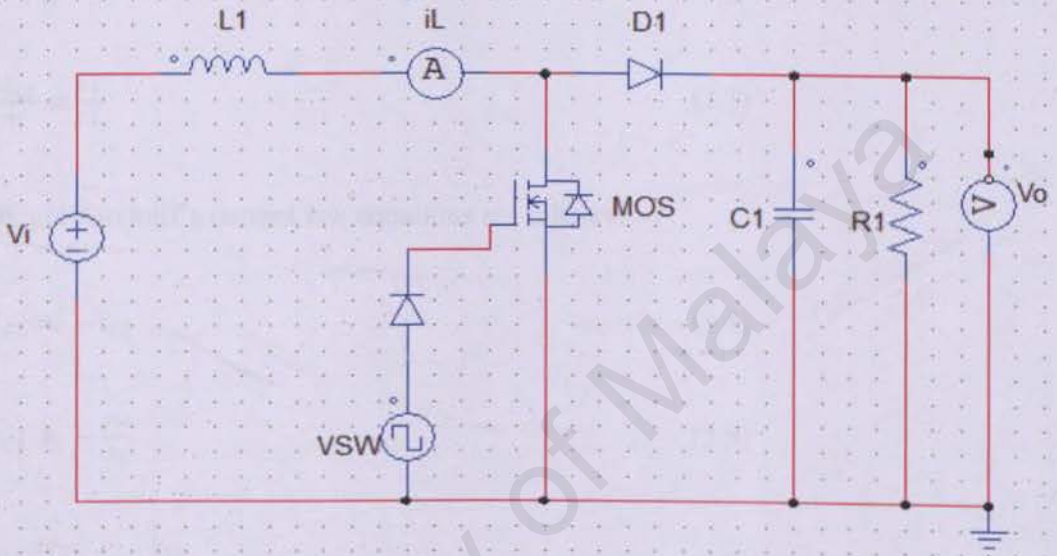


Figure 3.2: Boost converter circuit

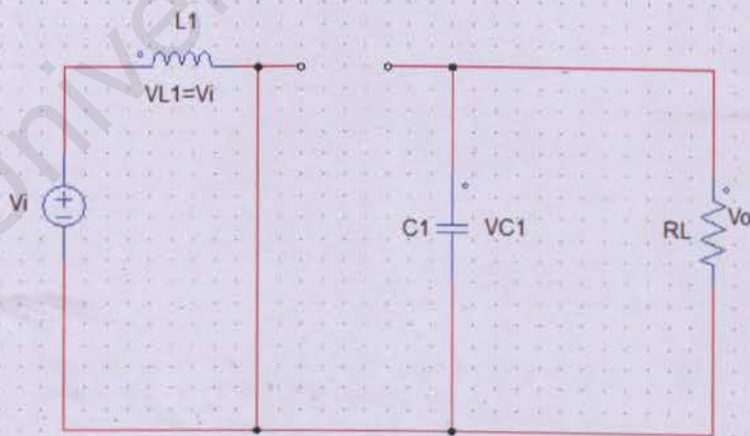


Figure 3.3: Boost converter when switched closed

A517447175

From Figure 3.3, Kirchoff's voltage law equation loops that can be derived are as follows (W. Hart, 2011).

$$V_{L1} = Vi \quad (3.1)$$

$$L1 \frac{di_{L1}}{dt} = Vi \quad (3.2)$$

$$\frac{di_{L1}}{dt} = \frac{Vi}{L1} \quad (3.3)$$

While Kirchoff's current law equations are follows:

$$i_{C1} = -i_{RL} \quad (3.4)$$

$$i_{C1} = -\frac{Vo}{RL} \quad (3.5)$$

$$C1 \frac{dV_{C1}}{dt} = -\frac{V_{C1}}{RL} \quad (3.6)$$

$$\frac{dV_{C1}}{dt} = -\frac{V_{C1}}{RL \cdot C1} \quad (3.7)$$

Following Figure 3.4 shows the operation of boost converter when it is switched open.

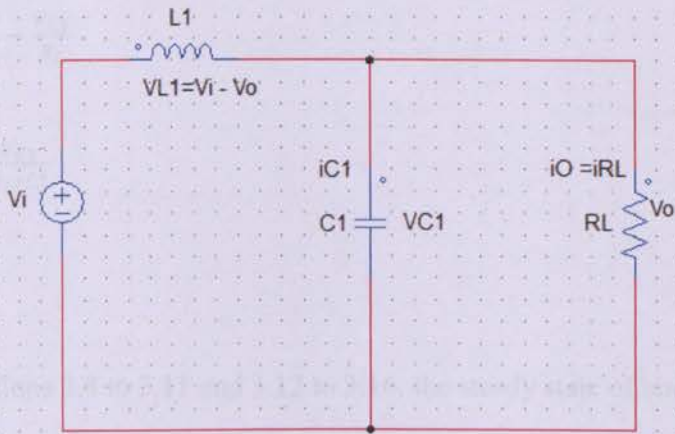


Figure 3.4: The boost converter when it is switched open

For the case when it is switched open, Kirchoff's voltage law equations are as follows

(W. Hart, 2011)

$$V_{L1} = V_i - V_o \quad (3.8)$$

$$V_{L1} = V_i - V_{C1} \quad (3.9)$$

$$L1 \frac{di_{L1}}{dt} = V_i - V_{C1} \quad (3.10)$$

$$\frac{di_{L1}}{dt} = \frac{V_i - V_{C1}}{L1} \quad (3.11)$$

Likewise, Kirchoff's current law equations are shown below (W. Hart, 2011)

$$i_{L1} = i_{C1} + i_o \quad (3.12)$$

$$i_{C1} = i_{L1} - i_o \quad (3.13)$$

$$i_{C1} = i_{L1} - \frac{V_0}{R_L} \quad (3.14)$$

$$C1 \frac{dV_{C1}}{dt} = i_{L1} - \frac{V_{C1}}{R_L} \quad (3.15)$$

$$\frac{dV_{C1}}{dt} = \frac{i_{L1}}{C1} - \frac{V_{C1}}{R_L * C1} \quad (3.16)$$

Thus, from Equations 3.8 to 3.11 and 3.12 to 3.16, the steady state of boost converter can be derived as follows (W. Hart, 2011)

$$\frac{di_{L1}}{dt} = \frac{V_i}{L1} (d) + \left[\frac{V_i - V_{C1}}{L1} \right] (1 - d) = \frac{V_i}{L1} - \frac{V_{C1}}{L1} (1 - d) \quad (3.17)$$

$$\frac{dV_{C1}}{dt} = -\frac{V_{C1}}{R_L * C1} (d) - \left[\frac{i_{L1}}{C1} - \frac{V_{C1}}{R_L * C1} \right] (1 - d) = \frac{i_{L1}}{C1} (1 - d) - \frac{V_{C1}}{R_L * C1} \quad (3.18)$$

Otherwise the above state can also be transformed into matrix as below which assume $(1 - d) = D$, (W. Hart, 2011)

$$\dot{x} = \begin{bmatrix} \frac{di_{L1}}{dt} \\ \frac{dV_{C1}}{dt} \end{bmatrix} \quad (3.19)$$

$$A = \begin{bmatrix} 0 & -\frac{D}{L1} \\ \frac{D}{C1} & -\frac{1}{R_L * C1} \end{bmatrix} \quad (3.20)$$

$$x = \begin{bmatrix} i_{L1} \\ V_{C1} \end{bmatrix} \quad (3.21)$$

$$B = \begin{bmatrix} \frac{V_i}{L1} \\ 0 \end{bmatrix} \quad (3.22)$$

For steady state operation, the net change in inductor current must be zero. The relationship between output voltage (V_o), input (V_i) and duty cycle (D) is (W. Hart, 2011);

$$\frac{V_o}{V_i} = \frac{1}{1-D} \quad (3.23)$$

The average current in the inductor is figured by (W. Hart, 2011)

$$i_{L1} = \frac{V_i}{(1-D)^2 R_L} \quad (3.24)$$

In order to find period (T):

$$T = \frac{1}{f} \quad (3.25)$$

Minimum and maximum inductor current are determined by using the average value and the change in current values (W. Hart, 2011).

$$I_{max} = \frac{V_i}{(1-D)^2 R_L} + \frac{V_i \cdot DT}{2 \cdot L1} \quad (3.26)$$

$$I_{max} = \frac{V_i}{(1-D)^2 R_L} - \frac{V_i \cdot DT}{2 \cdot L1} \quad (3.27)$$

The minimum combination of inductance and switching frequency for continuous current in the boost converter is represent in following equation (W. Hart, 2011)

$$L_{min} = \frac{D(1-D)^2 R_L}{2f} \quad (3.28)$$

The output voltage V_o is determined from equation (W. Hart, 2011)

$$V_o = V_{C1} \quad (3.29)$$

The above Equation 3.29 is valid for both switch positions, resulting in $C_1^T = C_2^T = C$

$$C = [0 \quad 1] \quad (3.30)$$

and

$$x = \begin{bmatrix} i_{L1} \\ V_{C1} \end{bmatrix} \quad (3.31)$$

3.4 Analyzing of state space modelling

Parameter used in the boost converter system are presented in Table 3.1.

Table 3.1: Boost converter circuit (Pallavi Behera1, 2015)

Parameters	Values
V_i	12.31V
V_o	24.27V
$L1$	100mH
$C1$	180 μ F
RL	50 Ω
f	50kHz

From the equation 3.23, duty cycle D can be calculated by inserting all related parameters required as follows:

$$\frac{V_o}{V_i} = \frac{1}{1-D}$$

$$D = 0.5$$

All parameters assigned for boost converter are exploited in identifying state space matrices, as depicted below

$$A = \begin{bmatrix} 0 & -\frac{D}{L1} \\ D & \frac{1}{R_L * C1} \end{bmatrix}$$

$$A = \begin{bmatrix} 0 & -\frac{0.5}{100m} \\ 0.5 & \frac{1}{(50)(180\mu)} \end{bmatrix}$$

$$A = \begin{bmatrix} 0 & -5 \\ 2.78k & -111.11 \end{bmatrix}$$

$$B = \begin{bmatrix} \frac{V_i}{L1} \\ 0 \end{bmatrix}$$

$$B = \begin{bmatrix} 123.1 \\ 0 \end{bmatrix}$$

$$C = [0 \quad 1]$$

The value of state space duty cycle, D is 0.5. Equation 3.24 is revisited to find the average current in the inductor.

$$i_{L1} = \frac{V_i}{(1-D)^2 R_L}$$

$$i_{L1} = 0.98A$$

Equation 3.25 is revisited to find the value of time period, T :

$$T = \frac{1}{f}$$

As mentioned before earlier, this converter is required to be operated in *Continuous Conduction Mode*, CCM. Therefore, both equation 3.26 and 3.27 are revisited and all parameters are substituted.

In order to find I_{max} ,

$$I_{max} = \frac{V_i}{(1-D)^2 R_L} + \frac{V_i * DT}{2 * L1}$$

$$I_{max} = 0.981 A$$

In order to find I_{min} ,

$$I_{max} = \frac{V_i}{(1-D)^2 R_L} - \frac{V_i * DT}{2 * L1}$$

$$I_{max} = 0.978 A$$

From the result collected, it shows that I_{max} and I_{min} do not reach zero, and this is acceptable proven that this boost converter is in CCM.

Equation 3.28 is revisited to check minimum combination of inductance and switching frequency for continuous current in the boost converter as shown below:

$$L_{min} = \frac{D(1-D)^2 R_L}{2f}$$

As stated in the circuit parameter information, value of inductor $L = 100\text{mH}$ is enough to meet boost converter specification since it is higher than the minimum requirement value $L_{min} = 62.5 \mu\text{H}$.

Up to this stage, all matrices needed for boost converter modelling have been successfully developed and this information is then used to verify controllability, observability as well as to determine location of the poles.

3.5 Analyzing of controllability

A boost converter is considered fully controllable if its Rank $[M_c] = 2$ or determinant $[M_c] \neq 0$. Hence, Equation 2.12 is revisited to confirm the controllability of the boost converter.

$$M_c = [B \quad AB]$$

$$AB = \begin{bmatrix} 0 & -5 \\ 2.78k & -111.11 \end{bmatrix} \begin{bmatrix} 123.1 \\ 0 \end{bmatrix}$$

$$AB = \begin{bmatrix} 0 \\ 342.22k \end{bmatrix}$$

$$M_C = \begin{bmatrix} 123.1 & 0 \\ 0 & 342.22k \end{bmatrix}$$

$$|M_C| = 42.13 \times 10^6$$

From the above equations, Rank $[M_C] = 2$ and $|M_C| = 42.13 \times 10^6 \neq 0$. These findings proved that controllability principles and requirement are met and thus concludes that boost converter is fully controllable.

3.7 Analysis of system transfer function

The transfer function of boost converter is defined by below equation

3.6 Analysis of observability

A boost converter is considered fully observable if its Rank $[M_o] = 2$ or determinant $[M_o] \neq 0$. Hence, Equation 2.34 is revisited to test the observability of a boost converter.

$$M_o = \begin{bmatrix} C \\ CA \end{bmatrix}$$

$$CA = [0 \quad 1] \begin{bmatrix} 0 & -5 \\ 2.78k & -111.11 \end{bmatrix}$$

$$CA = [2.78k \quad -111.11]$$

$$M_o = \begin{bmatrix} 0 & 1 \\ 2.78k & -111.11 \end{bmatrix}$$

$$|M_o| = -2.78k$$

From the above equations, it was shown that Rank $[M_o] = 2$ and $|M_o| = -2.78k \neq 0$. The result shows the observability principles and requirement. Hence, it can be concluded that the boost is fully observable. Apart from the above deployed methods, boost converter controllability check can also be performed by using Matlab® & Simulink software tools.

Since both controllability and observability of boost converter had been proven, both controller and observer are ready to be implemented on the boost converter. Therefore, as the next step in the analysis process, the poles location of the system will be obtained.

3.7 Analysis of poles location

Poles location or eigenvalues of boost converter is defined by below equations:

$$|sI - A| = 0$$

$$\begin{vmatrix} s & 0 \\ 0 & s \end{vmatrix} - \begin{bmatrix} 0 & -5 \\ 2.78k & -111.11 \end{bmatrix} = 0$$

$$s^2 + 111.11s + 13900 = 0$$

Then poles value are determined by using Matlab & Simulink software tools. Based on Matlab & Simulink calculation result, poles of boost converter are located at:

$$P_{1,2} = (-55.555 \pm 103.99i)$$

3.8 Calculation of state feedback controller

Pole placement and optimal control technique are presented in this project to retrieve gain value of state feedback controller.

3.9 Pole placement technique

Poles location for boost converter had been calculated in the previous step. Thus, in the s-plane, poles are located at $(-55.555 \pm 103.99i)$. There are altogether three groups of pole placement to be designed and compared the effect of pole placement more to the left in s-plane. They are Poles 150x, Poles 250x and Poles 350x. table 3.2 shows the details of the three groups of poles placements.

Table 3.2: Pole placement group

Poles group	Pole Placement	
	P1	P2
Poles 150x	-8333.25	-8333.25
Poles 250x	-13888.75	-13888.75
Poles 350x	-19444.25	-19444.25

The closed loop characteristic is recalled and Equation 3.26 is revisited to find the feedback controller gain matrix, K.

Where $k=[k_1 \quad k_2]$

$$|\lambda I - (A - BK)| = 0$$

$$\begin{vmatrix} s & 0 \\ 0 & s \end{vmatrix} - \begin{bmatrix} 0 & -5 \\ 2.78K & -111.11 \end{bmatrix} + \begin{bmatrix} 123.1 \\ 0 \end{bmatrix} [k_1 \quad k_2] = 0$$

$$s^2 + (111.11 + 123.1k_1)s + 13677.64k_1 + 342218k_2 + 13900 = 0$$

$k_1 + k_2$ characteristic equation of the new pole placement is determined by revisited Equation 2.17. hence poles at Poles 150x characteristic equation can be written as follows:

$$(s + 8333.25)(s + 8333.25)$$

$$s^2 + 16666.5s + 69.443 \times 10^6 = 0$$

Coefficient in Equation 3.32 and 3.33 are the compared to find value of k_1 and k_2 .

$$111.11 + 123.1k_1 = 16666.5$$

$$k_1 = 134.49$$

Next, substitute $k_1 = 134.49$ to find k_2 :

$$13677.64k_1 + 342218k_2 + 13900 = 69.443 \times 10^6$$

$$13677.64(134.49) + 342218k_2 + 13900 = 69.443 \times 10^6$$

$$k_2 = 197.54$$

The feedback gain for Poles 150x is as described below:

$$K = [k_1 \quad k_2] = [134.49 \quad 197.54]$$

The same approach is repeated to determine feedback gains for Poles 250x and Poles 350x. the gain $K1$, $K2$ and $K3$ are represented for *Poles 150x*, *Poles 250x* and *Poles 350x* respectively.

The feedback gain determined for each group is recorded in Table 3.3 as shown below:

Table 3.3: State feedback controller gain for designated pole placement

Poles group	State feedback controller gain, K	
	k_1	k_2
<i>Poles 150x (K1)</i>	134.49	197.54
<i>Poles 250x (K2)</i>	224.75	554.68
<i>Poles 350x (K3)</i>	315.01	1092.2

During this initial stage, all state feedback controller gains based on pole placement technique have been successfully calculated and recorded. The best compensated output voltage is then obtained from the best pole placement group. On that account, Matlab & Simulation tools are used to analyse the output voltage. In the coming sub section, calculation of state feedback controller gain based on optimal control technique is presented.

3.10 Optimal control technique

Linear quadratic cost function is recalled:

$$J = \int_0^{\infty} (x^T Q x + u^T R u) dt$$

On the other hand, matrix Q can be derived from:

$$Q = C^T C \quad (3.34)$$

Matrix C is substituted to determine matrix Q as depict in below equations,

$$Q = [0 \ 1]^T [0 \ 1]$$

$$Q = \begin{bmatrix} 0 \\ 1 \end{bmatrix} [0 \ 1]$$

$$Q = \begin{bmatrix} 0 & 0 \\ 0 & 1 \end{bmatrix}$$

Cost function is minimized by manipulating state and leaving input as default $R=[1]$.

Next, Equation (2.31) is recalled. Matrix P is then calculated by using Riccati equation and all related matrices are substituted:

$$A^T P + P A - P B R^{-1} B^T P + Q = 0$$

$$\begin{bmatrix} 0 & -5 \\ 2.78K & -111.11 \end{bmatrix}^T \begin{bmatrix} p_{11} & p_{12} \\ p_{21} & p_{22} \end{bmatrix} + \begin{bmatrix} p_{11} & p_{12} \\ p_{21} & p_{22} \end{bmatrix} \begin{bmatrix} 0 & -5 \\ 2.78K & -111.11 \end{bmatrix}$$

$$- \begin{bmatrix} p_{11} & p_{12} \\ p_{21} & p_{22} \end{bmatrix} \begin{bmatrix} 123.1 \\ 0 \end{bmatrix} [1]^{-1} \begin{bmatrix} 123.1 \\ 0 \end{bmatrix}^T \begin{bmatrix} p_{11} & p_{12} \\ p_{21} & p_{22} \end{bmatrix} + \begin{bmatrix} 0 & 0 \\ 0 & 1 \end{bmatrix} = 0$$

Matrix P is solved by using Matlab LQR function as depicted in below equation:

$$P = \begin{bmatrix} 4.6665 \times 10^{-2} & 5.9351 \times 10^{-3} \\ 5.9351 \times 10^{-3} & 11.8309 \times 10^{-3} \end{bmatrix}$$

Afterwards, Equation 2.22 is recalled to calculate state feedback controller gain based on optimal control technique. All parameters are substituted as shown below:

$$K = R^{-1} B^T P$$

$$K = [1]^{-1} \begin{bmatrix} 123.1 \\ 0 \end{bmatrix}^T \begin{bmatrix} 4.6665 \times 10^{-2} & 5.9351 \times 10^{-3} \\ 5.9351 \times 10^{-3} & 11.8309 \times 10^{-3} \end{bmatrix}$$

$$K = [5.7445 \quad 0.73061]$$

The K value can be determined by using Matlab m-file. It will be used in Matlab & Simulink software to analyze the output voltage.

3.11 Calculation of feed forward controller gain

The gain, K for this state feedback will still be using a pole placement technique. Therefore, in controller, $K3 = [315.01 \quad 1092.2]$ has been chosen as feedback gain. Once again Equation (2.23) is recalled to find out the Nx and Nu value.

$$\begin{bmatrix} Nx \\ Nu \end{bmatrix} = \begin{bmatrix} A & B \\ C & E \end{bmatrix}^{-1} \begin{bmatrix} 0 \\ 1 \end{bmatrix}$$

$$\begin{bmatrix} Nx \\ Nu \end{bmatrix} = \begin{bmatrix} 0 & -5 & 123.1 \\ 2.78k & -111.11 & 0 \\ 0 & 1 & 0 \end{bmatrix}^{-1} \begin{bmatrix} 0 \\ 0 \\ 1 \end{bmatrix}$$

$$\begin{bmatrix} Nx \\ Nu \end{bmatrix} = \begin{bmatrix} 3.9968 \times 10^{-2} \\ 1 \\ 4.0617 \times 10^{-2} \end{bmatrix}$$

$$Nx = \begin{bmatrix} 3.9968 \times 10^{-2} \\ 1 \end{bmatrix} \text{ and } Nu = 0.04$$

Finally, the N value is obtained after Equation 2.24 is revisited.

$$N = Nu + KNx$$

$$N = 0.04 + [315.01 \quad 1092.2] \begin{bmatrix} 3.9968 \times 10^{-2} \\ 1 \end{bmatrix}$$

$$N = 1104.8$$

The N value can also find from Matlab m-file. It will be used in Matlab & Simulink software to simulate and analyze the output voltage. As next step, the integral controller design will be analyzed.

3.12 Calculation of integral controller gain

Integral controller is implemented to eliminate external element by tracking the whole system feedback. Thus, the new gain K and N need to be obtained. Equation 2.37 and 2.39 are revisited to find the new matrix A and B before the new gain can be obtained. After Equation 2.29 is revisited, the new matrix A and B are obtained. After Equation 2.29 is revisited, the new matrix A and B are obtained in form:

$$\dot{x} = Ax + Bu$$

$$A = \begin{bmatrix} 0 & -5 & 0 \\ 2.78k & -111.11 & 0 \\ 0 & -1 & 0 \end{bmatrix}$$

$$B = \begin{bmatrix} 123.1 \\ 0 \\ 0 \end{bmatrix}$$

The new K is described as follows:

$$K = [k_1 \quad k_2 \quad -k_3]$$

$$K = [0.04513 \quad 8.1271 \times 10^{-7} \quad -0.22565]$$

As per explained in subchapter 2.9, both K and N values are written as,

$$K = [0.04513 \quad 8.1271 \times 10^{-7}]$$

$$N = -0.22565$$

Afterward, full state observer design will be analyzed as the next step.

3.13 Calculation of full state observer gain

In order to find observer, gain L, Equation 2.46 is recalled to determine characteristic equation of a full state observer.

$$|sI - (A - LC)| = 0$$

$$\begin{vmatrix} [s & 0] - [0 & -5] + [l_1] \\ [0 & s] - [2.78k & -111.11] + [l_2] \end{vmatrix} [0 \quad 1] = 0$$

$$s^2 + (111.11 + l_2)s + 13900 + 2.78kl_1 = 0$$

The characteristic equation of Poles 150x is given below:

$$(s + 8333.25)(s + 8333.25)$$

$$s^2 + 16666.5s + 69.443 \times 10^6 = 0$$

The characteristic equation of Poles 150x are compared to find l_1 and l_2 :

$$13900 + 2.78kl_1 = 69.443 \times 10^6$$

$$l_1 = 24978$$

$$111.11 + l_2 = 16666.5$$

$$l_2 = 1.6555 \times 10^4$$

The observer gain, L for Poles 150x is:

$$L = \begin{bmatrix} l_1 \\ l_2 \end{bmatrix} = \begin{bmatrix} 2.4978 \times 10^4 \\ 1.6555 \times 10^4 \end{bmatrix}$$

The observer gain matrix, L can also be computed by using Matlab & Simulink software.

The same method is repeated to determine the observer gains for Poles 250x and Poles 350x. the observer gain for each group is recorded in Table 3.4.

Table 3.4: Full state observer gain for designated pole placement

Full state observer gain, L	Pole Placement		
	Poles 150x	Poles 250x	Poles 350x
l_1	2.4978×10^4	6.9386×10^4	1.36×10^5
l_2	1.6555×10^4	2.766×10^4	3.8777×10^4

The full state observer gains are calculated, simulated and recorded. Matlab® & Simulink simulation is used to analyze output voltage of both boost converter controller as well as observer. However, only Poles 250x (l_2) is selected to be investigated as observer output result. After all, required values to design the controller and observer are successfully determined, the next step is run simulation of the controller and observer design.

3.14 Simulation block diagram

Once all components for the design are determined, design of boost converter controller and observer are tested by using Matlab® Simulink simulation application. Two kind of system activation are tested, namely *open loop system* and *closed-loop system*. Results obtained between the two system types are analysed and compared to find the one with the best characteristics.

3.14.1 Wind turbine system

Figure 3.5 is illustrated Simulink model of the wind turbine. There are three which is generator speed (w_r pu) in pu for the nominal speed of the generator, the pitch angle in degrees and the wind speed in m/s , the tip speed ratio of lambda, λ in pu of nominal lambda λ_{nom} is gained by the separation of the rational speed and the wind speed in pu of the base wind speed. The output is the torque applied to the generator shaft. The fixed wind speed is 12 m/s suitable for wind turbine system (Trejos-Grisales, 2014).

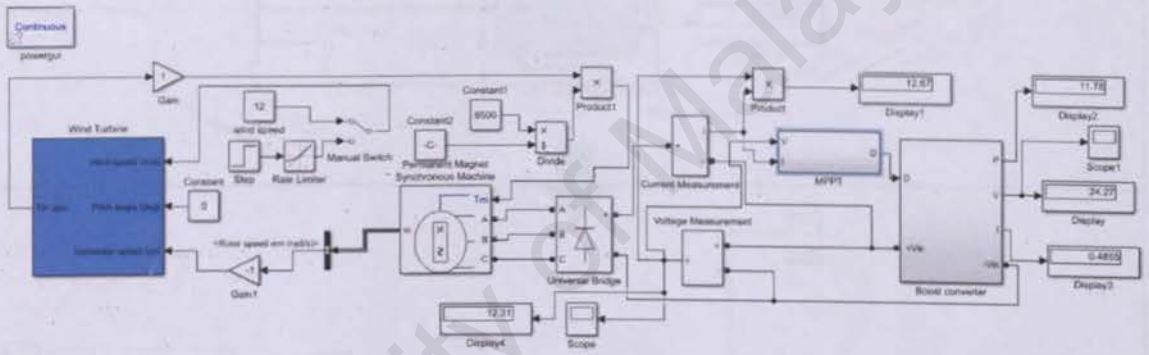


Figure 3.5: Simulink model of wind turbine system

Figure 3.6 illustrated the Simulink model for boost circuit from the wind turbine system in figure 3.5. The Simulink model for boost is come from the block in red dash at Simulink model at wind turbine.

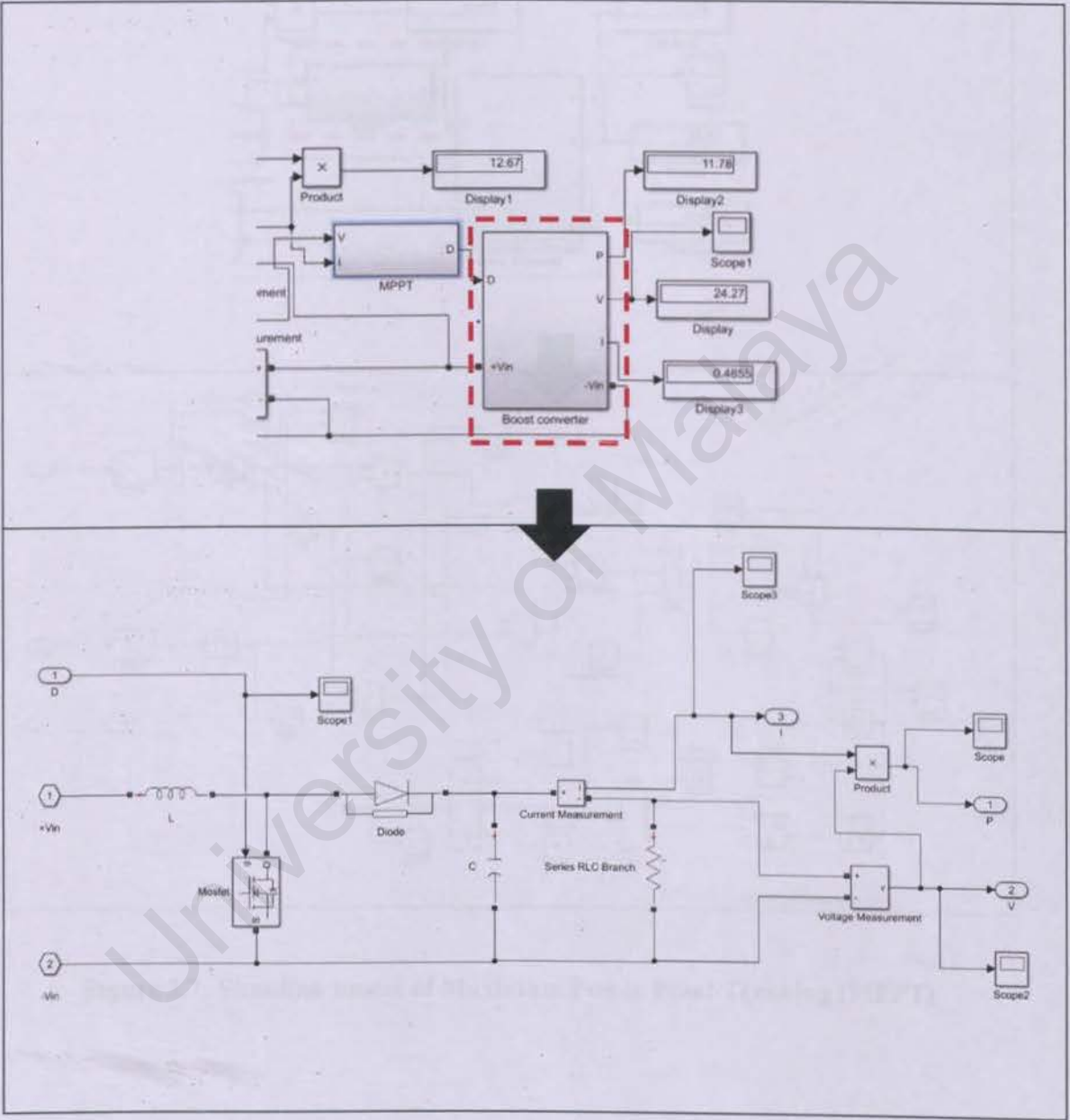


Figure 3.6: Simulink model of boost circuit

Figure 3.7 shows that Simulink of MPPT from the main Simulink model of wind turbine from figure 3.5. The red dash is the part of Simulink model for MPPT.

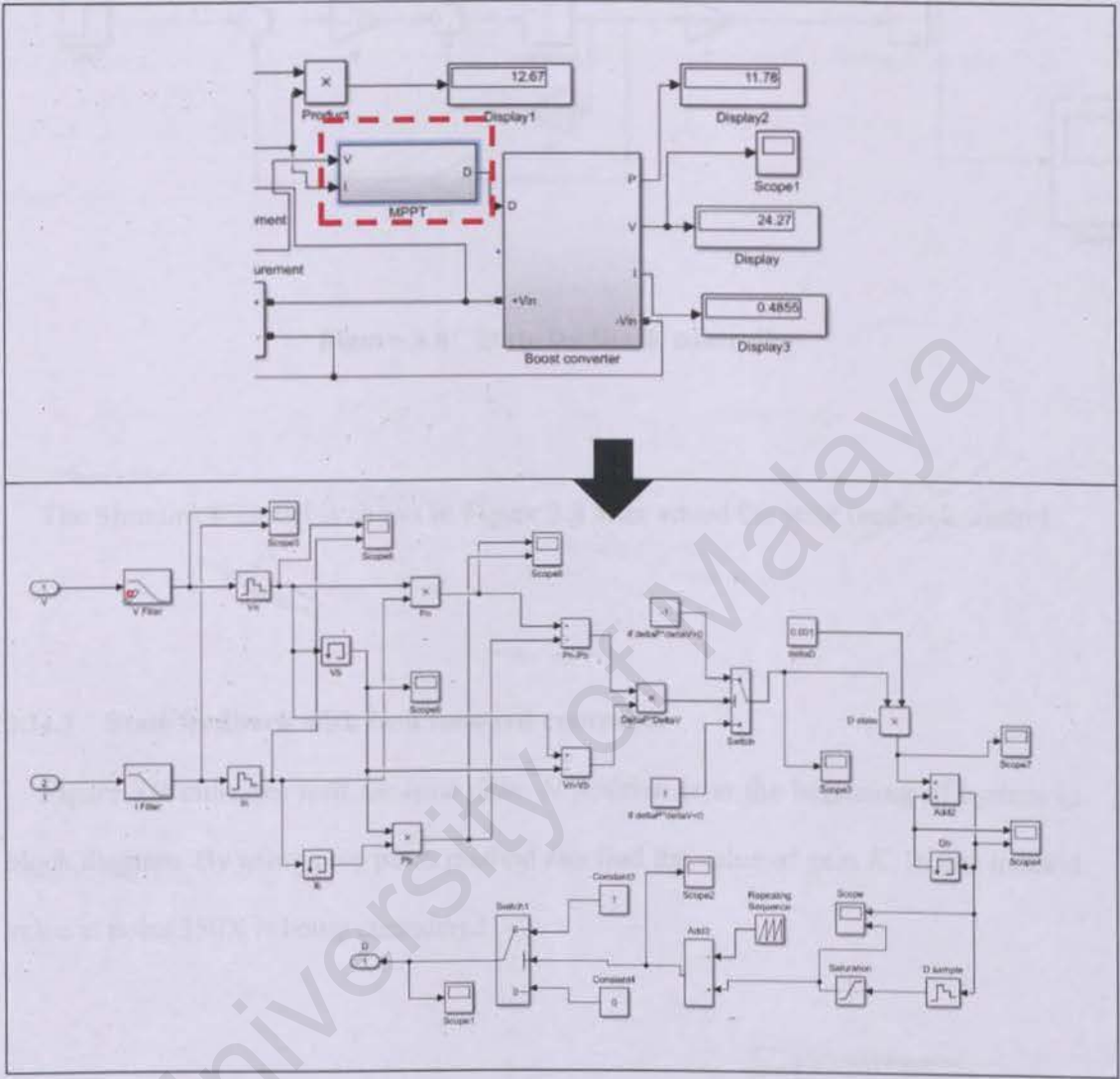


Figure 3.7: Simulink model of Maximum Power Point Tracking (MPPT)

3.14.2 State feedback controller

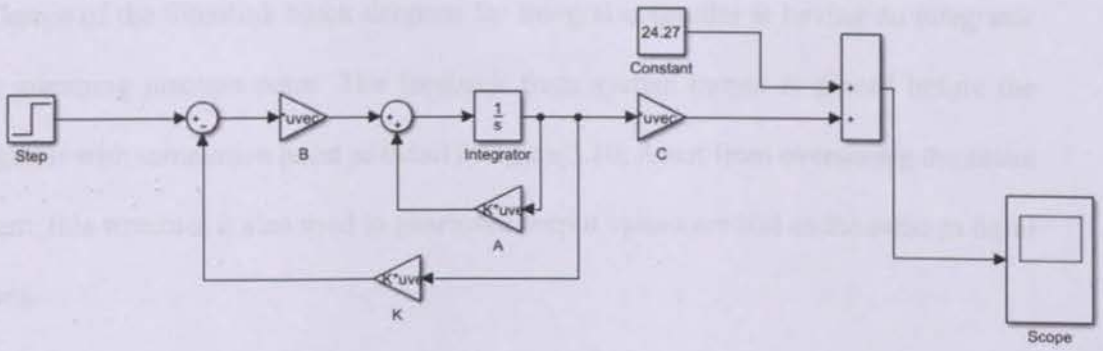


Figure 3.8: State feedback controller

The Simulink® model is shown in Figure 3.8 after adding the state feedback control

3.14.3 State feedback with feed forward controller

Figure 3.9 indicates *feed forward gain*, N position is at the beginning of the system in the block diagram. By using the pole placement method, the value of gain K can be found. In this method, the value at poles $350X$ is being considered.

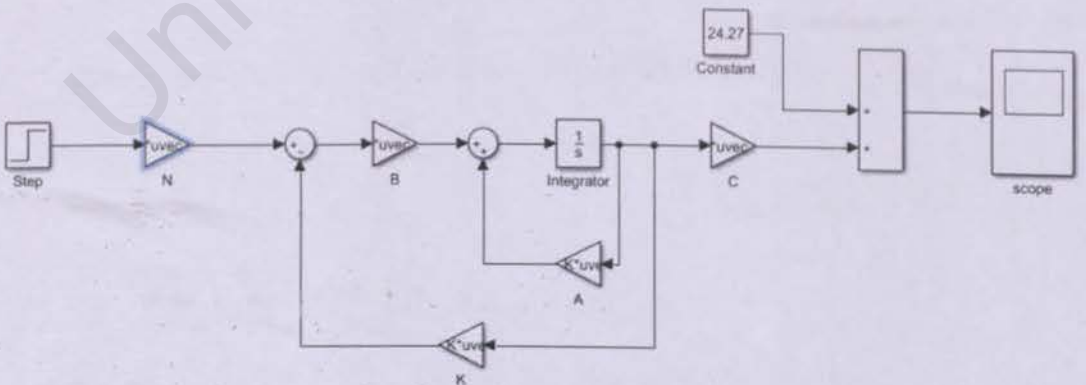


Figure 3.9: State feedback with feed forward controller

3.14.4 Integral controller

Design of the Simulink block diagram for integral controller is having an integrator after summing junction point. The feedback from system output is placed before the integrator with summation point as detail in figure 3.10, Apart from overseeing the entire system, this structure is also used to guarantee output values are still as the same as input values.

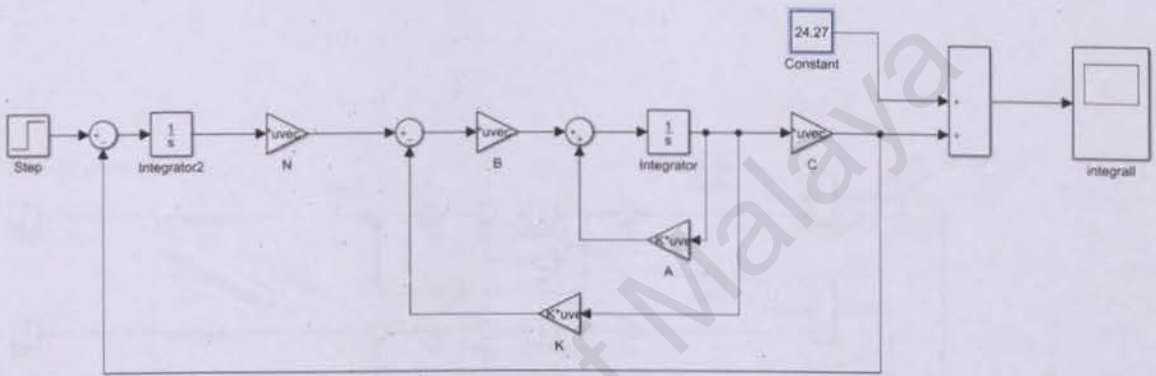


Figure 3.10: Integral controller

3.14.5 Comparison of modern controller

There are four types of controller that are involved for the comparison of modern controllers which are made up of state feedback controller, optimal controller, state feedback with feedforward controller and integral controller. The investigated modern controllers are combined in one single Simulink block diagram for a better comparison. The entire signals from each controller are displayed in the same scope. The configuration of Simulink block diagram is shown in Figure 3.11.

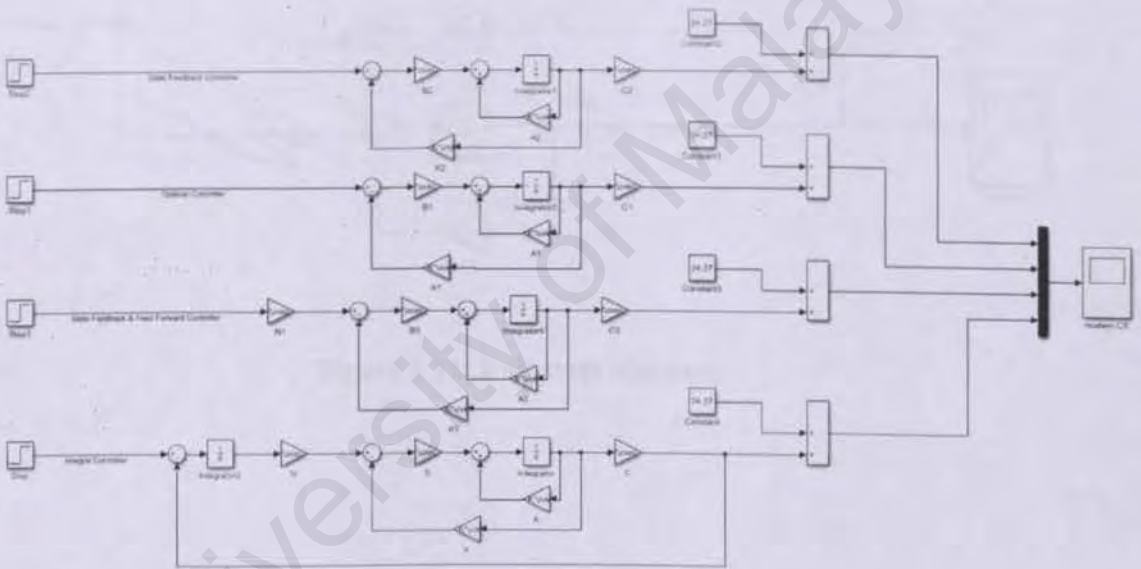


Figure 3.11: Comparison of modern controller

3.14.6 Full state observer

The combination of boost converter and full state observer in one block diagram is shown in Figure 3.12. The back-state value used in the feedback control are estimated via the full state observer. Output value measured at *Scope 1* must be equal with output value measured at *Scope 2*

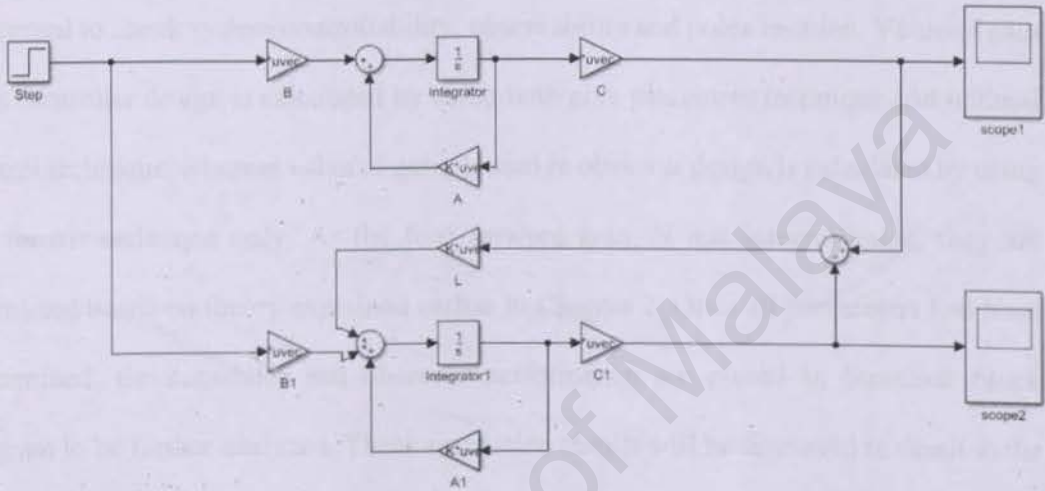


Figure 3.12: Full state observer

3.15 Summary

In the beginning of this chapter, flow chart is presented to summarize flow and procedure that take place within this project. Mathematical modelling shows that parameter applied on the system meet standard project requirement. The boost converter is designed to be presented in steady state form. Since it is required to be operated in CCM, minimum current of i_L need to be guaranteed. Boost converter state space model is derived to check system controllability, observability and poles location. Value of gain K in controller design is calculated by using both pole placement technique and optimal control technique, whereas value of gain, L used in observer design is calculated by using the former technique only. As the feed forward gain, N and integral value, they are calculated based on theory explained earlier in Chapter 2. Once all parameters had been determined, the controller and observer performance are placed in Simulink block diagram to be further analyzed. These simulation results will be discussed in detail in the following chapter together with further discussion of the boost converter and observer system.

CHAPTER 4: RESULT AND DISCUSSION

This chapter discusses on controller simulation results based on steady state, settling time, percentage of overshoot and steady-state error. Whilst, observer is investigating the developed observer with the original boost system of the output voltage.

4.1 Introduction

Table 4.1 listed that the requirement parameters of boost converter for designing purpose where input voltage V_i is set to 12.31V and the desired output voltage V_o is predictable 24.27V

Table 4.1: Requirement parameters of boost converter

Output voltage, V_o	24.27V
Input voltage, V_i	12.31V

4.2 Wind turbine system

Matlab® Simulink was used to simulate the wind turbine circuit. Simulation result of output voltage V_o of wind turbine boost converter model as shown in Figure 4.1.

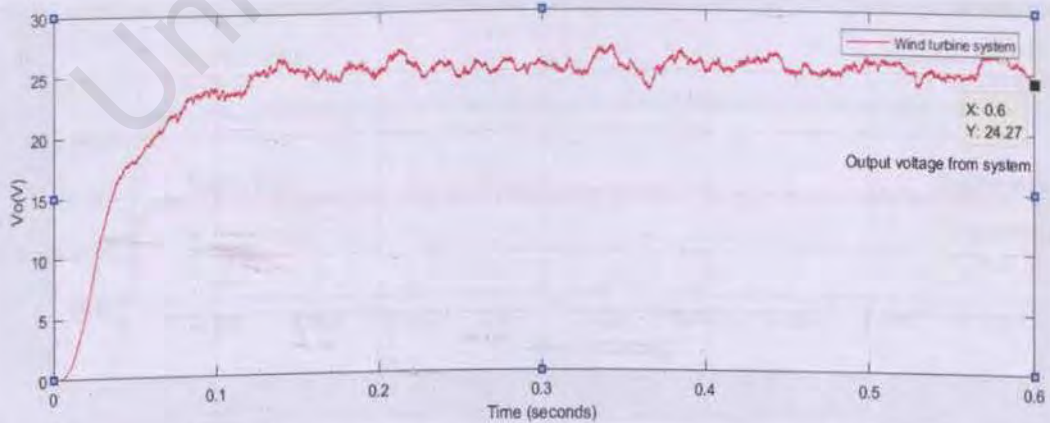


Figure 4.1: Wind turbine boost converter model.

From the graph collected in Figure 4.1, the result shows that voltage produced ripples, has slow settling time and high overshoot. Thus, improvements are implemented by designing and evaluating various modern controllers.

4.3 State feedback based on pole placement

State feedback controller can be implemented by applying two techniques, namely pole placement technique and optimal control technique. Derivation of state feedback controller gain, K for Simulink model had been explained earlier in Figure 3.8 by applying pole placement technique, gain value for $K1$ is inserted into K block diagram, and then followed by gain value $K2$ and $K3$ respectively. In the next page, output of three waveform appear in the same graph as shown in Figure 4.2.

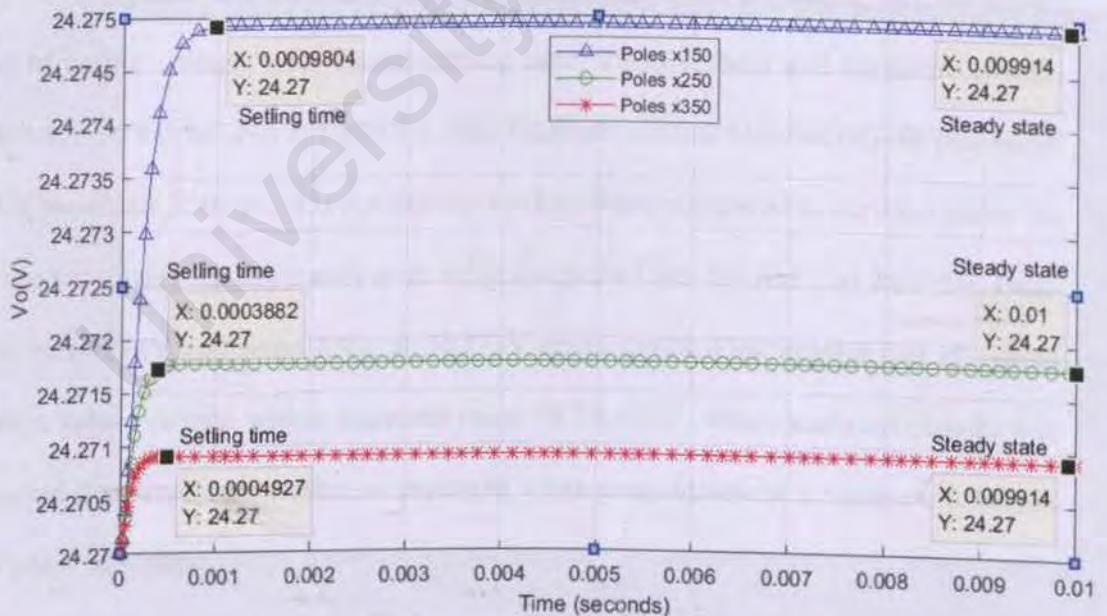


Figure 4.2: Poles placement technique results

Results collected from Figure 4.2 is summarized in Table 4.2 as shown below.

Table 4.2: Analysis result for pole placement technique

Pole location	Output voltage	Settling time	Overshoot (%)	Steady state error
Poles 150x (k1)	24.275	0.0009804	0	0.005
Poles 250x (k2)	24.272	0.0003882	0	0.002
Poles 350x (k3)	24.271	0.0004927	0	0.001

Results from the three poles are evaluated to find the best compensated output voltage. The best compensator should be a controller that is capable of producing 24.270v steady state of output voltage, with fastest settling time, 0% overshoot and minimum steady-state error. As can be seen in Table 4.2, state feedback controlled based on pole placement technique, Poles 250x provide the shortest settling times compared to the other poles. As the output voltage results, steady state value for poles 150x delivers it as 24.275V, Poles 250x at 24.272V and poles 350x at 24.271V respectively. This implies that all output voltage values remain within expected range of 24.270V. When analysed closely it is observed that steady state value is improved when poles locations are moved to the left half-plane in s-plane.

4.4 State feedback based on optimal control technique

Based on block diagram shown in Figure 3.6, the gain, K is determined by using Ricatti equation as derived earlier in subchapter 3.10. the simulation result by applying optimal controller is shown in Figure 4.3.

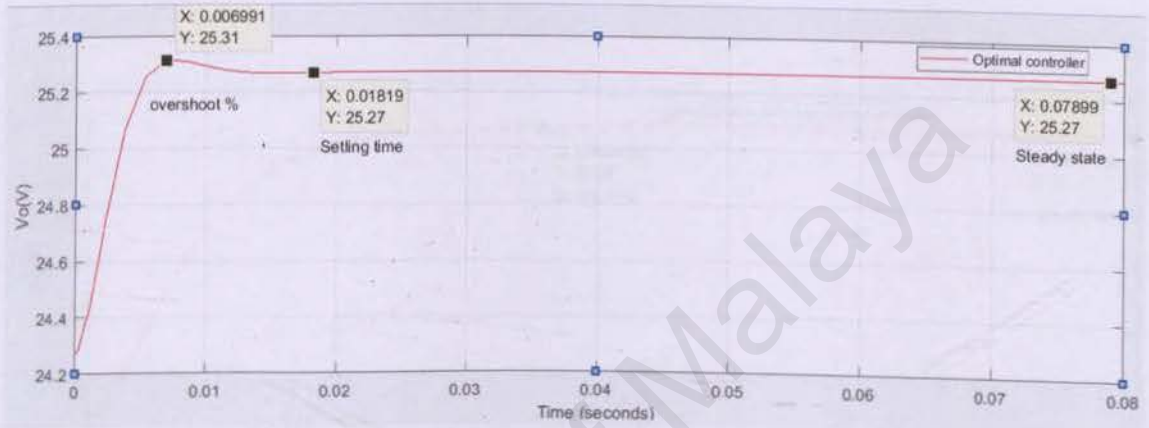


Figure 4.3: Optimal control technique results

From the graph illustrated above, it is shown that steady state of output voltage. V_o is 25.27 V while settling time. T_s is 0.01819 sec. Unfortunately, there is an overshoot of 0.212% occurred at 0.006991 sec which resulted a steady state error of 1V.

4.5 State feedback with feed forward controller

The block diagram for state feedback with feed forward controller is presented earlier in Figure 3.7. Based on that diagram, value of gain, K for poles $250x$ is chosen for this model, whereas the feed forward gain, N is calculated as explained in chapter 3.11. the result of this simulation is recorded in Figure 4.4 as shown below.

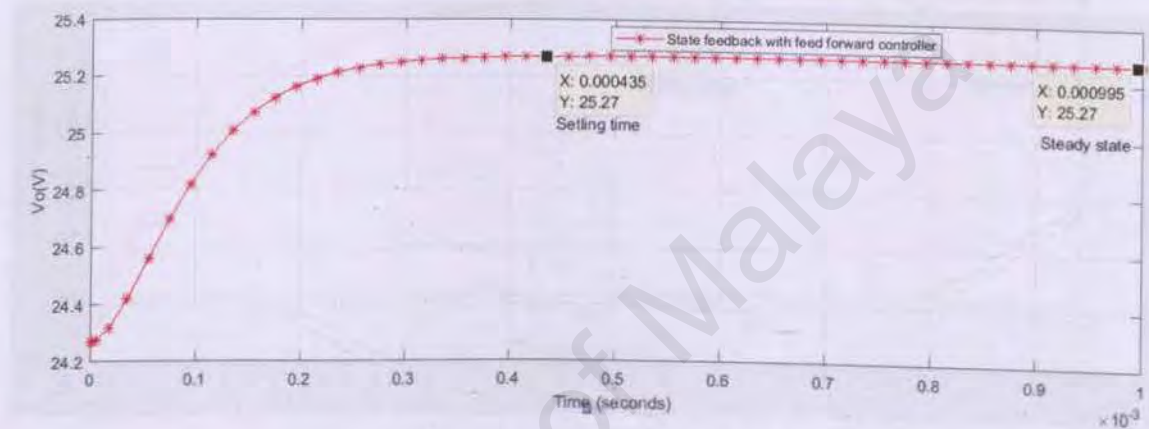


Figure 4.4: State feedback with feed forward controller results

As can be seen in the result, value of steady state output voltage has an additional 1V to make the value at 25.27V when compared to state feedback controller with Poles $250x$ and added feed forward gain, N . The additional 1V from the desired output voltage is possible because additional gain was inserted in front of the whole controller system but fortunately there is no overshoot at the output controller. It's settling time is also the fastest, at 0.000435 sec than T_s of optimal controller at, 0.01819 sec.

4.6 Integral controller

As illustrated in block diagram in Figure 3.10 the new gain, K and feed forward gain, N have been derived as described in subchapter 3.12. The simulation result of integral controller is detailed in Figure 4.5.

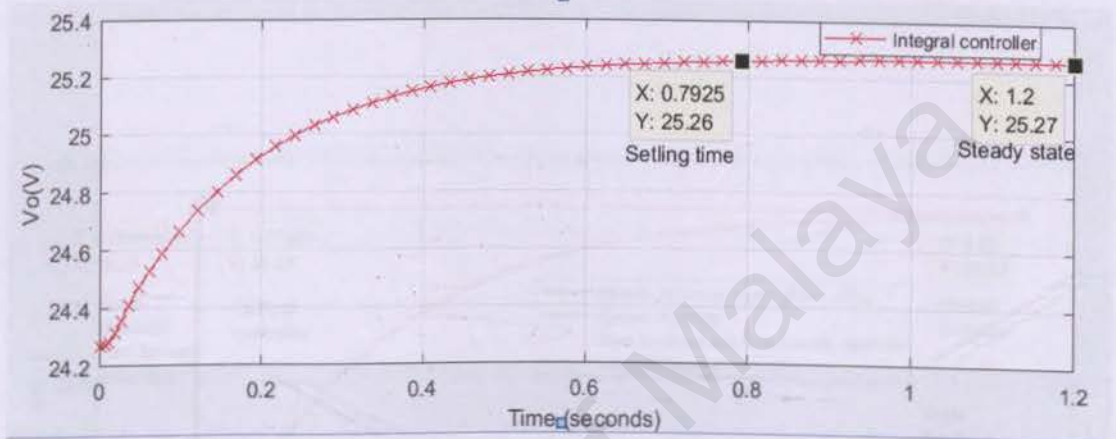


Figure 4.5: Integral controller result

Graph in figure 4.5 shows the steady state of the output voltage is at 25.27 with a settling time of 0.7925 sec. This is the slowest settling time as compared to all modern controllers that have been evaluated before. Besides that, this controller also produced 1V steady state error but with 0% overshoots. Furthermore, it can also be seen that the signal was degraded during rise time. The comparison of all modern controller results will be explained in the following section.

4.7 Comparison of modern controller

There are altogether four modern controllers involved in this comparison analysis. The output from each controller is presented in the same scope. For this purpose, the Simulink block diagram in figure 3.9 will be used as reference. The simulation result of the modern controller comparison is shown in Figure 4.6. The state feedback controller at poles 250x is obviously different others controller graphs because is the most accurate with set point.

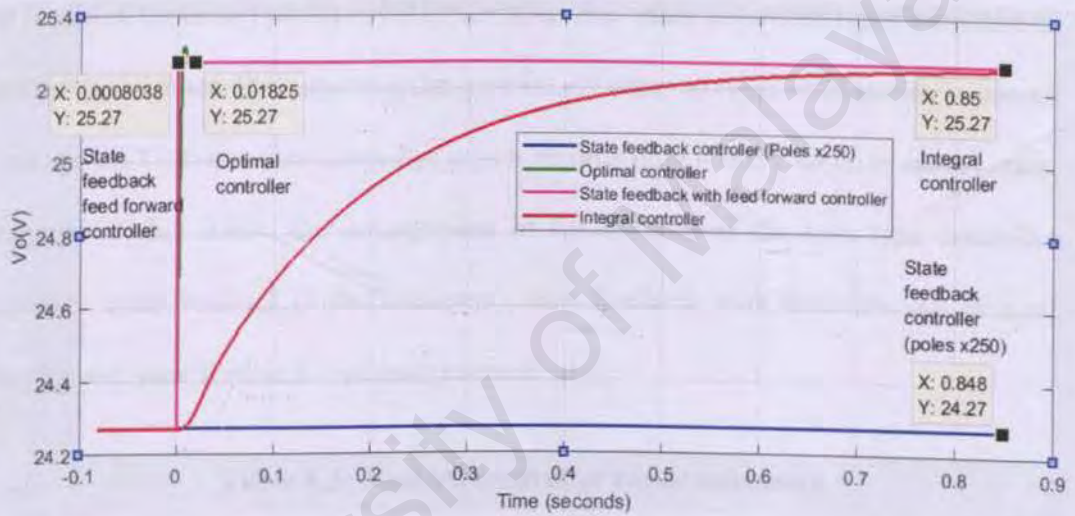


Figure 4.6: Comparison of modern controller

As illustrated in the result graph, all modern controllers achieve output voltage range of 24.272 to 25.270 V. However, the settling time, percentage of overshoot and steady-state error of the system needs to be considered separately in next section.

4.8 Result of modern controller

Table 4.3 shows the summary of the result of modern controller. By comparing four types of controller, the best result comes from state feedback pole placement at poles $250x$. It has achieved 0% overshoot and the lowest steady error is only 0.002V. Besides that, this type of controller also manages to accomplish the fastest settling time at 0.0003882 seconds. Meanwhile the settling time, T_s for state feedback (*optimal*), state feedback with feed forward and Integral controller are 0.01819 seconds, 0.000435 seconds and 0.7925 seconds respectively. Other than that, the overshoot only occurs at state feedback (*optimal*) which is 0.212%. Otherwise, other controller types recorded no overshoot occurrence. By respecting the error steady state, all types of controller achieved 1V except the best selection controller which records only 0.002V of error steady state. In regards of this result, the arrangement of the ranking of the best type controller selection is state feedback (Pole Placement), state feedback with feed forward, Integral controller and state feedback (*optimal*) respectively.

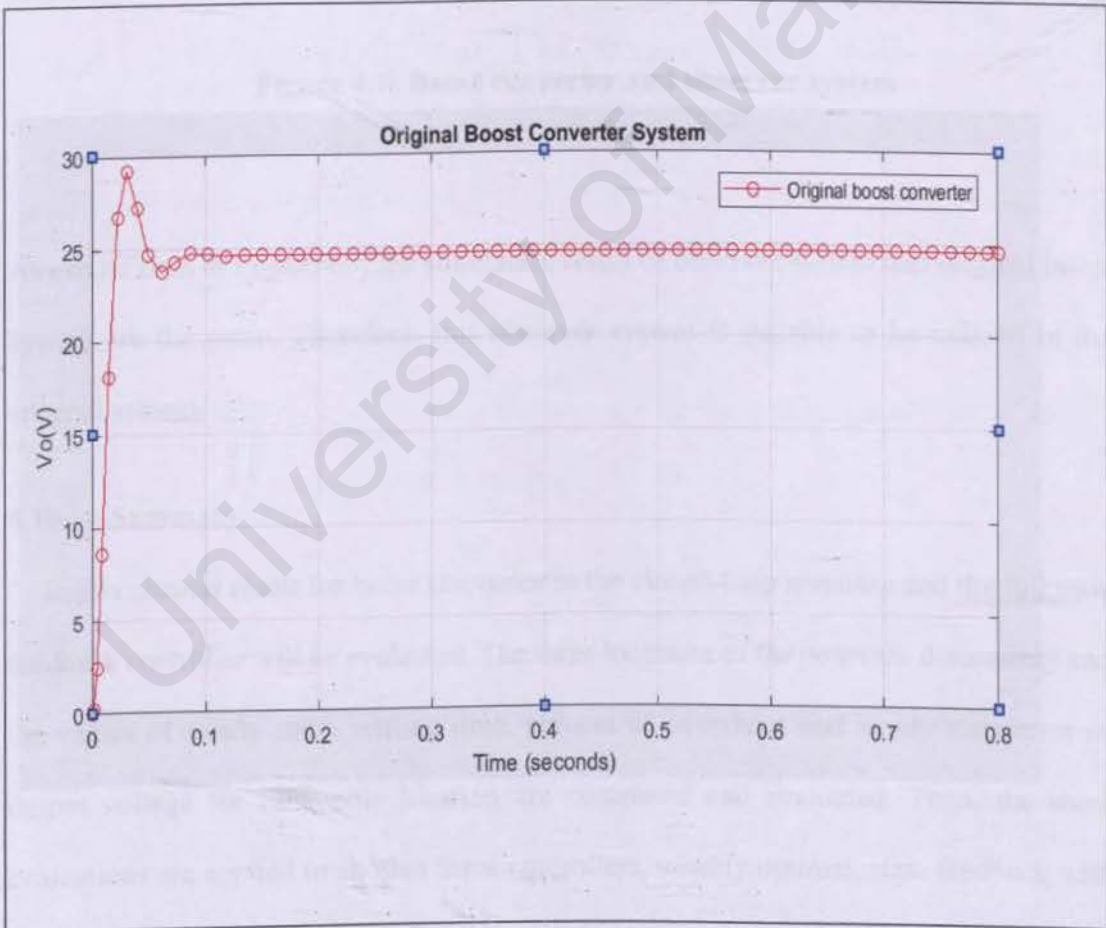
Table 4.3: Modern controller result summary

	State feedback (Pole Placement) Poles $250x$	State feedback (optimal)	State feedback with feed forward	Integral
Steady state(V)	24.272	25.270	25.270	25.270
Settling time T_s (sec)	0.0003882	0.01819	0.000435	0.7925
Overshoot (%)	0	0.212	0	0
Steady state Error (V)	0.002	1	1	1

4.9 Boost converter with full state observer simulation results

The expected result for observer output should be the same with the result of the open loop system. Before simulation started, gain value, L is calculated as described in subchapter 3.13 and inserted into the observer Simulink model to ensure it is comparable to the system output. The matrix gain L_2 selected to perform this observer evaluation is as shown below:

$$L_2 = \begin{bmatrix} l_1 \\ l_2 \end{bmatrix} = \begin{bmatrix} 69.386 \times 10^3 \\ 27.666 \times 10^3 \end{bmatrix}$$



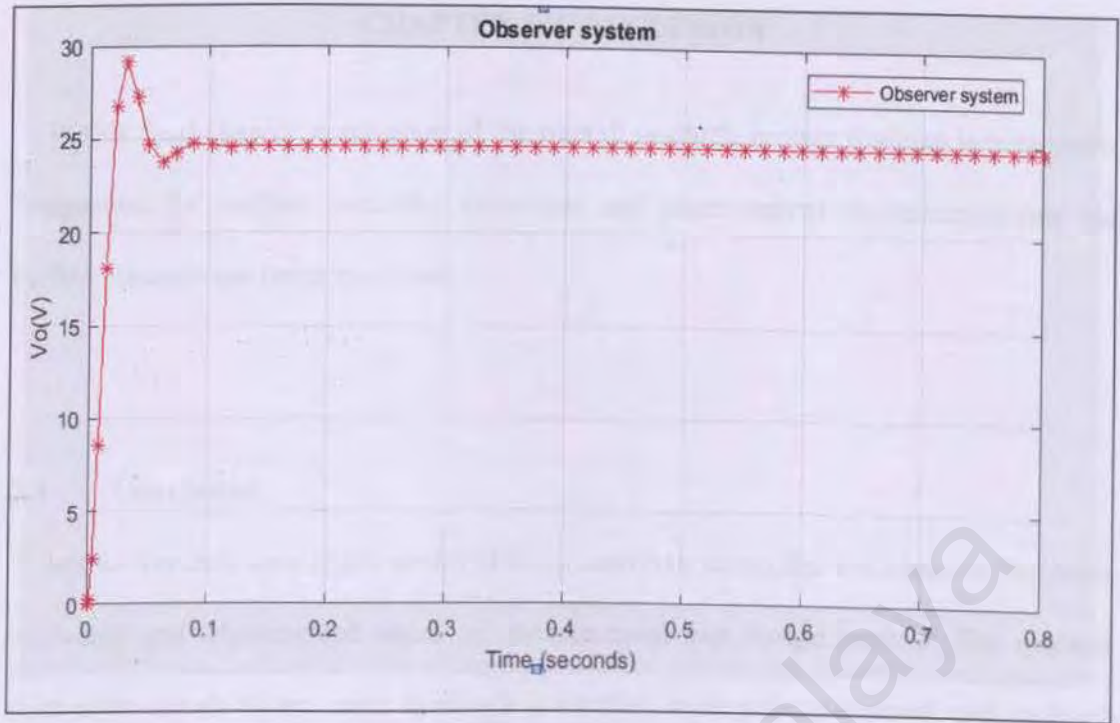


Figure 4.7: Boost converter and observer system

As can be seen in Figure 4.7, the simulation result of observer system and original boost system are the same. Therefore, this observer system is suitable to be utilized in the original system.

4.10 Summary

In this chapter result for boost converter in the closed-loop response and the full state feedback controller will be evaluated. The three locations of the poles are determined and the values of steady state, settling time, percent of overshoot and steady state error of output voltage for each pole location are compared and evaluated. Then, the same evaluations are applied to another three controllers, namely optimal, state feedback with feed forward and integral control. All the modern controller results are summarized in a table.

CHAPTER 5: CONCLUSION

In this final chapter, conclusion of the overall research project findings is presented. Suggestion for modern controller technique and improvement recommendations for further research are being specified.

5.1 Conclusion

In this research, state space model of boost converter controller and observer had been explained and implemented based on modern controller design method. The modern controllers involved are state feedback controller with pole placement and optimal method, state feedback with feed forward controller and integral controller. In this project, the input and output voltage were gained from the simulation of Maximum Power Point Tracking (MPPT) using boost converter for wind energy conversion system which is 24.27 V for output voltage and 12.31V for input voltage. All structured controllers are assessed by utilizing Matlab ® and Simulink ® programming devices. State space averaging procedure is connected to discover the state space matrix which is utilized in the reproduction of Simulink ® block diagram.

All objective of this project has been achieved successfully. Simulation models of various modern controllers and observer were effectively worked by utilizing Matlab ® and Simulink ® programming devices. Results accumulated from the simulations have helped in the performance evaluation process of each model. Furthermore, the best controller will be determined to be implemented in the boost converter system.

After evaluating all collected result, it is recommended to use state feedback controller based on pole placement technique such as shown by 250x since it provides the fastest settling time at 0.0003882 sec has smallest steady state error of 0.002 and 0% overshoot on output voltage.

5.2 Recommendation for future work

For further improvements, this proposal can be implemented on hardware with parameter values as acquired during simulation phase. The standard DC-DC boost converter is assembled with gain value, K inserted as feedback control. Prior to assembling the hardware parts, it is advisable to simulate involved circuits by using PSIM or Matlab ® & Simulink®.

REFERENCES

- Abdullah, M. A., Yatim, A. H. M., Tan, C. W., & Saidur, R. (2012). A review of maximum power point tracking algorithms for wind energy systems. *Renewable and Sustainable Energy Reviews*, 16(5), 3220-3227. doi: <https://doi.org/10.1016/j.rser.2012.02.016>
- Eviningsih, R. P., Putri, R. I., Pujiantara, M., Priyadi, A., & Purnomo, M. H. (2017, 25-27 March 2017). *Controlled bidirectional converter using PID for charging battery in the stand-alone wind turbine system with Modified P&O to obtain MPPT*. Paper presented at the 2017 International Conference on Green Energy and Applications (ICGEA).
- Jeong, H. G., Seung, R. H., & Lee, K. B. (2012). An Improved Maximum Power Point Tracking Method for Wind Power Systems. *Energies*, 5(5), 1339.
- Kumar, D., & Chatterjee, K. (2016). A review of conventional and advanced MPPT algorithms for wind energy systems. *Renewable and Sustainable Energy Reviews*, 55, 957-970. doi: <https://doi.org/10.1016/j.rser.2015.11.013>
- Odgaard, P. F., Hovgaard, T. G., & Wiesniewski, R. (2016, June 29 2016-July 1 2016). *Model predictive control for wind turbine power boosting*. Paper presented at the 2016 European Control Conference (ECC).
- Ogata, k. (2010). *Modern Control Engineering*. *Modern Control Engineering* (Vol. 17).
- Pallavi Behera, D. K. K. (2015). SIMULATION OF MPPT TECHNIQUE USING BOOST CONVERTER FOR WIND ENERGY CONVERSION SYSTEM. *International Journal of Advance Research In Science And Engineering*, Vol. No.4(Special Issue (01)).
- Singh, A., & Mirafzal, B. (2016, 18-22 Sept. 2016). *Three-phase single-stage boost inverter for direct drive wind turbines*. Paper presented at the 2016 IEEE Energy Conversion Congress and Exposition (ECCE).
- Trejos-Grisales, L., Guarnizo-Lemus, C., & Serna, S. (2014). Overall Description of Wind Power Systems. *Ingeniería y Ciencia*, 10, 99-126.
- Vinod, A., & Sinha, A. K. (2014, 13-14 Feb. 2014). *A study on intelligent algorithms for maximum power point tracking in field of wind energy conversion system (review)*. Paper presented at the 2014 International Conference on Electronics and Communication Systems (ICECS).
- W. Hart, D. (2011). *Power Electronics*. New York: McGraw-Hill.

Yaramasu, V., Wu, B., Sen, P. C., Kouro, S., & Narimani, M. (2015). High-power wind energy conversion systems: State-of-the-art and emerging technologies. *Proceedings of the IEEE*, 103(5), 740-788. doi: 10.1109/JPROC.2014.2378692

University of Malaya